

This discussion paper is/has been under review for the journal Atmospheric Chemistry and Physics (ACP). Please refer to the corresponding final paper in ACP if available.

**Vapour isotopic
composition in
updrafts**

M. Bolot et al.

Modelling and interpreting the isotopic composition of water vapour in convective updrafts

M. Bolot¹, B. Legras¹, and E. J. Moyer²

¹Laboratoire de Météorologie Dynamique, CNRS/ENS, UMR8539, Paris, France

²Department of the Geophysical Sciences, University of Chicago, Chicago, USA

Received: 10 May 2012 – Accepted: 14 June 2012 – Published: 31 August 2012

Correspondence to: M. Bolot (bolot@lmd.ens.fr)

Published by Copernicus Publications on behalf of the European Geosciences Union.

Title Page

Abstract

Introduction

Conclusions

References

Tables

Figures

◀

▶

◀

▶

Back

Close

Full Screen / Esc

Printer-friendly Version

Interactive Discussion



Abstract

The isotopic compositions of water vapour and its condensates have long been used as tracers of the global hydrological cycle, but may also be useful for understanding processes within individual convective clouds. We review here the representation of processes that alter water isotopic compositions during processing of air in convective updrafts and present a unified model for water vapour isotopic evolution within undiluted deep convective cores, with a special focus on the out-of-equilibrium conditions of mixed phase zones where metastable liquid water and ice coexist. We use our model to show that a combination of water isotopologue measurements can constrain critical convective parameters including degree of supersaturation, supercooled water content and glaciation temperature. Important isotopic processes in updrafts include kinetic effects that are a consequence of diffusive growth or decay of cloud particles within a supersaturated or subsaturated environment; isotopic re-equilibration between vapour and supercooled droplets, which buffers isotopic distillation; and differing mechanisms of glaciation (droplet freezing vs. the Wegener-Bergeron-Findeisen process). As all of these processes are related to updraft strength, droplet size distribution and the retention of supercooled water, isotopic measurements can serve as a probe of in-cloud conditions of importance to convective processes. We study the sensitivity of the profile of water vapour isotopic composition to differing model assumptions and show how measurements of isotopic composition at cloud base and cloud top alone may be sufficient to retrieve key cloud parameters.

1 Introduction

Because the relative abundances of the stable isotopologues of water – HDO, H₂¹⁸O, and H₂O – are sensitive to phase changes that occur within air masses, water isotopic ratios have long been used as tracers of the atmospheric water cycle (since pioneering works in the 1950s, see Dansgaard, 1964 for review). Although the primary motivation

ACPD

12, 22451–22533, 2012

Vapour isotopic composition in updrafts

M. Bolot et al.

Title Page

Abstract

Introduction

Conclusions

References

Tables

Figures

◀

▶

◀

▶

Back

Close

Full Screen / Esc

Printer-friendly Version

Interactive Discussion



Vapour isotopic composition in updrafts

M. Bolot et al.

Title Page

Abstract

Introduction

Conclusions

References

Tables

Figures

◀

▶

◀

▶

Back

Close

Full Screen / Esc

Printer-friendly Version

Interactive Discussion

for isotopic studies in the past has been the interpretation of paleoclimatic measurements (Jouzel and Merlivat, 1984, and references herewith), a second motivation is to obtain otherwise unretrievable information about convective processes (Jouzel et al., 1975; Risi et al., 2008; Lee et al., 2009; Kurita et al., 2011). Constraining convective processes has been a major incentive for recent efforts to include water isotopologues in General Circulation Models (Joussaume et al., 1984; Schmidt et al., 2005; Bony et al., 2008). These modelling studies, along with the recent availability of satellite observations of the isotopic composition of water vapour (Moyer et al., 1996; Kuang et al., 2003; Nassar et al., 2007; Steinwagner et al., 2007; Worden et al., 2011), have shown the potential of using water isotopologues to test our understanding of large-scale atmospheric processes (Risi et al., 2008; Lee et al., 2009). At smaller scales, in-situ measurements and inclusion of water isotopologues in cloud-resolving models may bring insight into the deep convective transport of water to the Tropical Tropopause Layer (TTL) (Smith et al., 2006; Hanisco et al., 2007; Blossey et al., 2010; Sayres et al., 2010). The isotopic signature of free tropospheric water vapour in the tropics and subtropics is, however, largely determined by processes within convective clouds and by the evaporation of condensates formed within convective clouds (Wright et al., 2009).

In the tropics, deep convection carries water vapour from the boundary layer upwards across isentropes to the free troposphere, where the budget of water vapour is then set by a balance between this convective moistening and drying by diabatic subsidence (Folkins and Martin, 2005). Large-scale stirring also redistributes water vapour towards the subtropics, moving it upwards along isentropes (Pierrehumbert and Roca, 1998; Couhert et al., 2010). Above ~ 15 km, in the TTL, slow diabatic ascent lofts dehydrated water vapour and further dehydrates air as it crosses the cold point along its trajectory (Fueglistaler et al., 2009). The dispersion in water vapour isotopic composition among GCMs and the discrepancies between models and observations are largest in the upper troposphere in these regions (Risi et al., 2012), and may result from missing processes or assumptions made in cloud parameterizations.

Vapour isotopic composition in updrafts

M. Bolot et al.

Title Page

Abstract

Introduction

Conclusions

References

Tables

Figures

◀

▶

◀

▶

Back

Close

Full Screen / Esc

Printer-friendly Version

Interactive Discussion



Our ability to model the convective transport of isotopologues can only be as good (or as bad) as our understanding of basic physical processes in convective clouds. As air parcels rise within convective clouds, they experience a wide range of thermodynamic conditions that drive transformations between the different phases of water. A minimal isotopic model needs to consider the fractionation of isotopologues between vapour, cloud water, rainwater, cloud ice and snow (i.e. airborne and precipitating species). Non-equilibrium behavior will occur whenever the speed of phase transformations is too slow for changes in saturation vapor pressure, i.e. whenever supersaturation exists: in rapidly rising convective systems, and in that temperature range where cloud water and cloud ice coexist. Under such conditions, fractionation processes are limited by diffusion of water vapour and heat. In a full treatment, droplet and cloud ice size distributions would also be taken into account, since the kinetic effects in isotopic fractionation between cloud water and vapour depend on droplet size, and the evaporation of droplets or ice crystals is size-dependent. (In this work we consider only unimodal particle size distributions).

Much of the material discussed in this paper has already been treated in the literature, and the basic physics of isotopologues is not new. Studies of isotopologues in the context of convection can be traced back to the pioneering works of Jouzel et al. (1975) and Federer et al. (1982). Further contributions to the field include Gedzelman and Arnold (1994); Moyer et al. (1996); Bony et al. (2008); Lee et al. (2009) and Blossey et al. (2010). Our aim here is to provide a consistent picture of how isotopic distributions are linked to cloud microphysics and thermodynamics, incorporating elements that are spread across several studies. We will also revisit some current assumptions on the representation of microphysics. In particular, we are interested in the effects related to saturation and glaciation on the distribution of isotopologues within deep convective clouds, which may open a way to retrieve quantitative informations on these key processes from isotopic observations. This work is motivated by the recent surge of field measurements in the upper troposphere (Sayres et al., 2009; Nassar et al., 2007; Steinwagner et al., 2007; Randel et al., 2012) and by rising interest in using

isotopologues to uncover cloud processes and their impact on tropical variability. For example, water isotopologues have recently been used to study the origin of water and circulations around clouds in hurricanes (Fudeyasu et al., 2008; Lawrence and Gedzelman, 1996, 2003) and the Madden-Julian oscillation (Kurita et al., 2011; Berkelhammer et al., 2012). A consistent model can aid interpretation of measurements and can be useful in helping to structure measurement programs.

In this paper, we describe and discuss a minimal model that predicts the isotopic composition of water vapour within convective clouds. We restrict the model based on two assumptions that limit its use to the study of deep convection. First, we omit any interaction between airborne and precipitating species. This assumption does not invalidate treatment of water vapour in updrafts, since precipitating condensates tend to be collected in convective-scale downdrafts that are spatially distinct from updrafts (see, e.g. LeMone and Zipser, 1980; Kirkpatrick et al., 2009). The model is thereby restricted to transformations between vapour, cloud water, and cloud ice. Second, we assume that those transformations are adiabatic (i.e. that entrainment is negligible). Entrainment and mixing properties would require further knowledge of the environment and are therefore not considered in this work. The modelling framework we present therefore best represents undiluted deep convection that reaches the upper troposphere (i.e. tropical hot towers, Riehl and Malkus, 1958; Fierro et al., 2009). These limitations do not hamper our ability to investigate how variations in updraft physics trigger variations in the distribution of vapour isotopologues within clouds.

In what follows, Sect. 2 reviews the well-known physics of fractionation and the kinetic effects induced by the diffusional growth of droplets and crystals; Sect. 3 describes the bulk approach to modelling and derives the equation governing the water vapour isotopic profile; Sect. 4 discusses model results for the distillation of water vapour as an air parcel ascends and its sensitivity to saturation and other microphysical processes; Sect. 5 discusses the comparative evolution of the $\text{H}_2\text{O}/\text{HDO}$ and $\text{H}_2\text{O}/\text{H}_2^{18}\text{O}$ systems; Sect. 6 evaluates the use of combined observation of HDO and H_2^{18}O to retrieve key convective parameters; and Sect. 7 summarises and offers further discussion.

Vapour isotopic composition in updrafts

M. Bolot et al.

Title Page

Abstract

Introduction

Conclusions

References

Tables

Figures

◀

▶

◀

▶

Back

Close

Full Screen / Esc

Printer-friendly Version

Interactive Discussion



2 Fractionation physics

This section reviews the basic physics of isotopes partitioning at microphysical scales and its connection with the macroscopic description of cloud physics. We describe notation (Sect. 2.1), review equilibrium isotopic partitioning (Sect. 2.2), and then turn to additional fractionation induced by the kinetics of particle growth/decay in Sect. 2.3. Additional material on kinetic effects is included in appendices: Appendix A reviews the representation of growth and loss rates of droplets and ice crystals that is the basis of the isotopic kinetic effects and Appendix B provides the full derivation of kinetic fractionation factors. We follow closely the derivations of Jouzel et al. (1975) and Jouzel and Merlivat (1984), but emphasize the differences between fractionation of ice and liquid water and highlight interpretations that are specific to the context of deep convection. Reviews covering similar material include Gedzelman and Arnold (1994) and Blossey et al. (2010).

2.1 Isotopic notation

Isotopic abundances are typically described in terms of isotopic ratios, e.g. for the deuterated water $R = [D]/[H]$ (or $R = \frac{1}{2} [HDO]/[H_2O]$). These isotopic ratios are themselves typically reported as per mil deviations from a standard: $\delta = 1000 \left(\frac{R}{R_0} - 1 \right)$, where R_0 is the isotopic ratio of the standard. (The symbols δD and $\delta^{18}O$ are used for the isotopic abundances of deuterium and oxygen 18 in water vapour, respectively). For water isotopologues, the reference standard is generally the Vienna Sea Mean Oceanic Water (V-SMOW) (Hagemann et al., 1970; Gonfiantini, 1978; Stichler et al., 1995). In this work, we have found it convenient to define isotopic ratio as the ratio of isotopologue masses rather than as the ratio of their abundances. That is, $R = \rho_{HDO}/\rho_{H_2O} = 2\rho_D/\rho_H$ or $R = \rho_{H_2^{18}O}/\rho_{H_2O} = \rho_{^{18}O}/\rho_{^{16}O}$, where the $\rho_{[...]}$'s represent densities of heavy and light isotopologues. Our definition leaves δ s unaffected, given an adjustment of the definition of R_0 (see Appendix C2). Fractionation factors (defined

Vapour isotopic composition in updrafts

M. Bolot et al.

Title Page

Abstract

Introduction

Conclusions

References

Tables

Figures

◀

▶

◀

▶

Back

Close

Full Screen / Esc

Printer-friendly Version

Interactive Discussion



below) are also unaffected by our definition. In what follows, we represent the heavy isotopologue quantity (HDO or H_2^{18}O) by a prime letter, e.g. $R = \rho' / \rho$.

2.2 Equilibrium fractionation

The vapour pressure isotope effect is a quantum phenomenon that results from a lowering of vibrational energies upon substitution of an atom by its heavy isotope equivalent (Herzfeld and Teller, 1938; Urey, 1947; Bigeleisen, 1961; Van Hook, 1968). At phase equilibrium between liquid and solid, or vapour and solid, the condensed phase is then relatively enriched in heavy isotopologues. This equilibrium partitioning is described, the equilibrium fractionation factors $\alpha_{l,i} = R_{l,i} / R_v \geq 1$ where R_v , R_l and R_i are, respectively, the isotopic ratios of vapour, liquid and ice. (The double index l,i is used here and in the sequel as a shorthand notation for relations which are valid for liquid water and ice). The fractionation factor $\alpha_{l,i}$ is a physical parameter that depends only on temperature, and is larger at colder temperatures (see Fig. 1 and Eq. C3).

Achieving this thermodynamic equilibrium fractionation requires that vapour surrounding cloud droplets or crystals be exactly at saturation, with no temperature contrast between environment vapour and condensates. In real-world cloud conditions, these conditions are unlikely to hold. First, condensates grow and evaporate under supersaturated or subsaturated environments. Second, growth and evaporation typically occur rapidly enough that condensate surfaces are not in thermodynamic equilibrium with their environments. Isotopic models must therefore be built on a broader kinetic theory, where thermodynamic equilibrium behaviour applies only at the surface of droplets or ice crystals, which interact with ambient air through a diffusive boundary layer. Under stationary conditions, this combination yields a pseudo-equilibrium between condensates and the environment. We describe this pseudo-equilibrium in the next section.

Vapour isotopic composition in updrafts

M. Bolot et al.

Title Page

Abstract

Introduction

Conclusions

References

Tables

Figures

◀

▶

◀

▶

Back

Close

Full Screen / Esc

Printer-friendly Version

Interactive Discussion



2.3 Kinetic fractionation factor and isotopic relaxation time for droplets and ice

Kinetic modifications to fractionation factors occur whenever phase transformations do not happen at thermodynamic equilibrium. Such effects were first discussed for ocean evaporation by Dansgaard (1964) and Craig and Gordon (1965), and were later investigated in the context of cloud physics by Gedzelman and Lawrence (1982) and Jouzel and Merlivat (1984).

Cloud droplets and crystals may grow from a supersaturated environment when the surrounding vapour field cannot adjust to saturation over liquid water or ice (as may happen when temperature and pressure drop is rapid and nuclei are limited. See for instance Korolev and Mazin, 2003). Conversely, droplets in the supercooled regime may evaporate in a subsaturated environment owing to liquid–ice thermodynamic disequilibrium. In supersaturated (resp. subsaturated) conditions, heavy and light vapour molecules diffuse toward the condensate (resp. away from it) across a boundary layer that connects the condensate surface to the far field environment, and the latent heat of phase transformation is extracted from the condensate (resp. imported to it) through a corresponding thermal boundary layer. The details of such processes are reviewed in Appendix A.

As a result of diffusive exchanges, the surface values of vapour density ($\rho_v^{(s)}$), temperature ($T^{(s)}$) and vapour isotopic ratio ($R_v^{(s)} = \rho_v'^{(s)} / \rho_v^{(s)}$) differ from those in the far field environment ($\rho_v^{(\infty)}$, $T^{(\infty)}$ and $R_v^{(\infty)} = \rho_v'^{(\infty)} / \rho_v^{(\infty)}$)¹. Gradients in both light and heavy water vapour isotopologues develop across the boundary layer. These gradients are necessarily different owing to preferential condensation and lower diffusivity of heavy isotopologues (Merlivat, 1978). Hence $R_v^{(\infty)} < R_v^{(s)}$ at droplet evaporation, and $R_v^{(\infty)} > R_v^{(s)}$ at droplet condensation or ice deposition, as illustrated in Figs. 2 and 3. One may

¹The environment beyond the diffusive boundary layer is also the far field from the point of view of diffusive theory (see Appendix A), hence the superscript (∞).

Vapour isotopic composition in updrafts

M. Bolot et al.

Title Page

Abstract

Introduction

Conclusions

References

Tables

Figures

◀

▶

◀

▶

Back

Close

Full Screen / Esc

Printer-friendly Version

Interactive Discussion



define kinetic fractionation factors between condensate surface and far field vapour ($\alpha_{k|l,i} = R_{l,i}^{(s)}/R_v^{(\infty)}$) that differ from the equilibrium fractionation factors that actually govern partitioning between condensate surface and surface vapour ($\alpha_{l,i} = R_{l,i}^{(s)}/R_v^{(s)}$).

The kinetic fractionation factors for liquid – vapour and ice – vapour phase transition are determined by coupling the laws of diffusion for heat, light vapour and heavy vapour (the full derivation is performed in Appendix B, see also Jouzel and Merlivat, 1984 and Ciais and Jouzel, 1994). This yields a common expression for α_{kl} and α_{ki} :

$$\alpha_{k|l,i} \equiv \frac{R_{l,i}^{(s)}}{R_v^{(\infty)}} = \frac{\alpha_{l,i}}{1 + (\beta_{l,i} - 1) \left(1 - (S_{l,i}^{(\text{eff})})^{-1}\right)}, \quad (1)$$

where

$$S_{l,i}^{(\text{eff})} = \left(1 - A_{l,i} \left(1 - S_{l,i}^{-1}\right)\right)^{-1}$$

is the effective saturation of vapour over liquid or ice measured at surface temperature $\rho_v^{(\infty)}/\rho_{\text{sat}}^{l,i} \left[T^{(s)}\right]$, $S_{l,i}$ is vapour saturation at far field temperature $\rho_v^{(\infty)}/\rho_{\text{sat}}^{l,i} \left[T^{(\infty)}\right]$, and $A_{l,i}$ are coefficients that represent the thermal impedance to condensate growth or evaporation (see Appendix A and Eq. A6 for definition). The $\beta_{l,i}$ are the product of the equilibrium fractionation factors $\alpha_{l,i}$ by the ratio of light to heavy isotopologue molecular diffusivities K_v/K_v' and the ratio of light to heavy isotopologue ventilation coefficients f_v/f_v' (see Appendix A and Supplement): $\beta_{l,i} = \alpha_{l,i} \frac{K_v f_v}{K_v' f_v'}$.

A crucial difference when deriving α_{kl} and α_{ki} comes from the fact that small droplets fully reequilibrate isotopically with the surrounding vapour (i.e. we wrote $\alpha_{kl} = R_l/R_v^{(\infty)}$, R_l referring to the whole droplet, and the assumption is $R_l^{(s)} \equiv R_l$) while ice does not reequilibrate because of the very slow migration of molecules within the crystal lattice (fractionation occurs only between ice surface and vapour: $\alpha_{ki} = R_i^{(s)}/R_v^{(\infty)}$).

Vapour isotopic composition in updrafts

M. Bolot et al.

Title Page

Abstract

Introduction

Conclusions

References

Tables

Figures

◀

▶

◀

▶

Back

Close

Full Screen / Esc

Printer-friendly Version

Interactive Discussion



Vapour isotopic composition in updrafts

M. Bolot et al.

Title Page

Abstract

Introduction

Conclusions

References

Tables

Figures

◀

▶

◀

▶

Back

Close

Full Screen / Esc

Printer-friendly Version

Interactive Discussion



Under supersaturated conditions, fractionation during droplet growth or ice deposition is reduced relative to the equilibrium scenario (i.e. $\alpha_{k|i,i} > \alpha_{l,i}$ when $S_{l,i}^{(eff)} < 1$) (and vice versa, so that fractionation is enhanced under subsaturated conditions). That is, the sign of $\alpha_{k|i,i} - \alpha_{l,i}$ is opposite to that of $S_{l,i}^{(eff)} - 1$. This results because $\beta_{l,i}$ are always larger than 1: equilibrium fractionation factors $\alpha_{l,i}$ are always > 1 ; heavy isotopologues have higher diffusivity than light ones so that $K_v/K'_v > 1$; and f_v/f'_v is close to unity. (See Appendix C5 for discussion of diffusivities and Supplement for ventilation coefficients.) If the ambient environment is exactly at effective saturation ($S_{l,i}^{(eff)} = 1$), there is no diffusion limitation and no kinetic isotope effects occur: the kinetic fractionation factors reduce to $\alpha_{k|i,i} = \alpha_{l,i}$.

Mathematically, these kinetic isotopic effects arise from $\beta_{l,i} \neq 1$. It is important to recognise that such effects are due not only to differences in diffusivity (i.e. $K_v/K'_v > 1$) but also to the preferential uptake of heavy isotopologues at the droplet or ice surface (i.e. $\alpha_{l,i} > 1$). Both effects contribute to producing a gradient in isotopic composition between particle surface and its environment, and kinetic effects would arise even in the absence of differential diffusion. For H_2O/HDO , equilibrium fractionation at droplet or ice surface is a larger contributor to kinetic processes than is differential diffusivity since $K_v/K'_v \sim 1.03$ and $\alpha_i > \alpha_1 \sim 1.1$ even at Earth's surface temperatures and increases further with altitude. For $H_2O/H_2^{18}O$, both effects contribute more equally: the diffusivity ratio is again $K_v/K'_v \sim 1.03$ but equilibrium fractionation is only $\alpha_{l,i} \sim 1.02 - 1.05$. This difference makes evolution of the oxygen isotopologue system more sensitive to vapour saturation $S_{l,i}$.

Kinetic effects on fractionation are somewhat reduced by thermal impedance effects at deposition or evaporation, which themselves are a function of diffusion: i.e. to the fact that $S_{l,i}^{(eff)} \neq S_{l,i}$. Thermal impedance limits both vapour subsaturation at evaporation (i.e. $S_{l,i} < S_{l,i}^{(eff)} < 1$) and vapour supersaturation at deposition (i.e. $1 < S_{l,i}^{(eff)} < S_{l,i}$). Thermal impedance therefore reduces the kinetically modified increase of fractionation at evaporation and the decrease of fractionation at deposition. The effects of thermal

impedance decrease with reduced temperature and so are less important with altitude (see Appendix A for discussion).

Most isotopic modeling treatments assume that cloud droplets instantly equilibrate with their surrounding vapour. (In some cases, partial re-equilibration is considered for falling raindrops of large size). However, we show in Appendix B that even for cloud droplets, full equilibration does not necessarily occur at low temperatures and high up-draft speeds. Only a part of cloud liquid water, the smaller droplets, would be expected to fully equilibrate with surrounding vapour, with the non-equilibrating portion increasing at low temperatures (see also discussion in Sect. 4.1).

While a detailed tracking of isotopic imbalance between droplets and their surrounding vapour would require integrating an equation for the tendency on droplet isotopic ratio (see Eq. B3) over a spectrum of droplet sizes, we choose a simplified approach here. We separate droplets into two classes: “cloud water”, which comprises only those droplets that exchange heavy isotopologues with vapour rapidly enough (i.e. droplets are small enough) to fully re-equilibrate with their surroundings, and the remaining droplets (larger than the critical radius discussed in Appendix B), which do not adjust locally with vapour and are treated as passive regarding isotopologue exchanges. The second class of droplets are effectively isolated from the vapour whatever their subsequent evolution within the parcel (i.e. whether they precipitate or not). As droplets both grow and are brought to lower temperatures, they are converted from actively exchanging droplets to passive ones (represented as a simple auto-conversion process). Thermal relaxation times in droplets, by contrast, are always considerably smaller than isotopic relaxation times (Appendix A, Fig. ??). This contrast justifies the use of a steady-state solution of the heat transfer equation in deriving the evolution of droplet and vapour isotopic ratios.

Finally, we note one factor omitted in our framework that may be of importance for ice crystal isotopic evolution. We have assumed conditions of thermodynamic equilibrium at the surface of both droplets and ice crystals (i.e. $\rho_v^{(s)} = \rho_{\text{sat}}^{l,i} [T^{(s)}]$, $R_l^{(s)} = \alpha_l R_v^{(s)}$ and $R_i^{(s)} = \alpha_i R_v^{(s)}$). This assumption is reasonable for droplets of sufficient size that surface

Vapour isotopic composition in updrafts

M. Bolot et al.

Title Page

Abstract

Introduction

Conclusions

References

Tables

Figures

⏪

⏩

◀

▶

Back

Close

Full Screen / Esc

Printer-friendly Version

Interactive Discussion



curvature and salt molarity effects are negligible. However, it is less obviously appropriate for ice crystals. Surface kinetic processes are known to be of importance in crystal growth, which cannot be accurately described by simple capacitance models (Kuroda, 1984). Because slight supersaturations at crystal surface appear necessary to overcome surface kinetics, deposition coefficients for heavy and light isotopologues may differ, inducing additional fractionation effects. Theories of isotopic fractionation incorporating surface kinetic effects are only recently under development (DePaolo, 2011; Nelson, 2011) and we cannot include them here. However, ice crystal shapes suggest that at high supersaturations, crystal growth may be compatible with a pure diffusional theory and surface kinetics effects are less important.

3 Modelling isotopic composition

3.1 Bulk approach

In this section, we lay out a basic model of water vapour isotopic ratio in rising convective clouds. In order to come to a closed-form solution, bulk modelling of heavy and light isotopologues with several classes of water species is required, together with energy conservation. The previous sections described fractionation between vapour and single droplets or ice crystals; here we represent the interactions between vapour, cloud water and cloud ice in convective clouds. We describe of those bulk phases and their isotopologue content in terms of mass mixing ratios r_v , r_l , r_i and the corresponding isotopic ratios $R_v = r'_v/r_v$, $R_l = r'_l/r_l$ and $R_i = r'_i/r_i$. Conditions during parcel ascent are assumed to be stationary and all variables therefore depend on z only.

As mentioned previously, we separate cloud liquid into “cloud water”, smaller droplets that isotopically re-equilibrate with vapour, and larger droplets that are passive in terms of isotopic exchanges. We handle transformations between from the active to the passive class (droplet deactivation) as an auto-conversion process. Since the typical critical radii for deactivation are less than $50\ \mu\text{m}$ (cf. Appendix B), less than the

Vapour isotopic composition in updrafts

M. Bolot et al.

Title Page

Abstract

Introduction

Conclusions

References

Tables

Figures



Back

Close

Full Screen / Esc

Printer-friendly Version

Interactive Discussion



Vapour isotopic composition in updrafts

M. Bolot et al.

Title Page

Abstract

Introduction

Conclusions

References

Tables

Figures

◀

▶

◀

▶

Back

Close

Full Screen / Esc

Printer-friendly Version

Interactive Discussion



size of precipitating droplets within fast convective updrafts (Houze, 1993, chap. 3.1.3), droplets likely reach the onset of deactivation before the onset of precipitation in fast updrafts, while the reverse might be true in slow updrafts. Once droplets enter into the passive class, their subsequent evolution (i.e. whether they fall as precipitation or not) no longer affects water vapour isotopic evolution. The droplets auto-conversion process in our model therefore represents either precipitation or droplet deactivation, depending on which process is fastest in depleting the population of active droplets. (For completeness of the representation, we also define an auto-conversion process for cloud ice that represents actual precipitation, and a class of precipitating ice, but all ice is assumed to be non-exchanging with vapour).

Since we use an exact adiabatic assumption for the conservation of energy, our model requires that total water be conserved. In order to satisfy the adiabatic assumption while representing the isotopic isolation of deactivated/precipitated droplets, we track the deactivated/precipitated species in the water budget instead of treating them as sinks. The total light water and heavy isotopologue contents are then:

$$r_t = r_v + r_l + r_i + r_l^{(p)} + r_i^{(p)}, \quad (2)$$

$$r'_t = r'_v + r'_l + r'_i + r'_l^{(p)} + r'_i^{(p)}, \quad (3)$$

where deactivated/precipitated species are denoted as $x^{(p)}$.

The different kinetic properties for liquid water and ice have important consequences for bulk quantities. In the case of liquid water, the homogenization and rapid equilibration with a common environment for the active cloud water component insures that, in the bulk sense:

$$\frac{r'_l}{r_l} = \frac{(dr'_l/dt)}{(dr_l/dt)} = \alpha_{kl} \frac{r'_v}{r_v}.$$

That is, the fractionation factor partitions isotopologues between bulk vapour and (active) bulk liquid. (Because the kinetic fractionation coefficients previously defined

relate properties of the condensed phase with those of vapour beyond the diffusive boundary layer, we no longer need to distinguish between surface and far field quantities, and can therefore unambiguously remove the parenthesized superscripts (∞) or (s) introduced in the previous section unless surface quantities are explicitly required).

5 In the case of ice, we assume, consistently with our definition of α_{ki} , that crystal size or shape have no effect on isotopic fractionation, so that the partitioning between isotopologues in the bulk vapour and the surface of ice crystals is simply:

$$\frac{(dr'_i/dt)}{(dr_i/dt)} = \alpha_{ki} \frac{r'_v}{r_v}.$$

10 Note that the bulk composition r'_i/r_i is generally different from $(dr'_i/dt)/(dr_i/dt)$. The value of r'_i/r_i depends strongly of the history of the accumulation of ice in each crystal, and likely also differs for each crystal size in a distribution.

In the following subsections we first (Sect. 3.2) present a simple representation of the microphysics and thermodynamics of rising air parcels, considering light water alone. Second (Sect. 3.3), we apply the previously established isotopic relationships to extract
15 the evolution of the isotopic ratios of the various water species, in particular that of vapour (R_v).

3.2 Microphysics and thermodynamics

3.2.1 Thermodynamics

20 In the model presented here, we assume adiabatic thermodynamics in the rising air parcel, so that the ice-liquid water potential temperature θ_{il} is conserved (Tripoli and Cotton, 1981; Bryan and Fritsch, 2004). This assumption is equivalent to assuming perfect conservation of total entropy for dry air and all water species, and therefore precludes entrainment of environmental air. The adiabatic assumption thus limits the utility of the model to the cores of deep convection, that arguably do not entrain, or

Vapour isotopic composition in updrafts

M. Bolot et al.

Title Page

Abstract

Introduction

Conclusions

References

Tables

Figures

◀

▶

◀

▶

Back

Close

Full Screen / Esc

Printer-friendly Version

Interactive Discussion



to cores embedded within mesoscale convective systems that are plausibly somewhat isolated from their broader environment.

For strict adiabaticity (and conservation of θ_{il}) to hold, total water must be conserved and transformations must be reversible. As explained in the previous section, total water conservation is enforced by retaining deactivated/precipitated species within the parcel under the $(l^{(p)})$ and $(i^{(p)})$ water classes. The assumption of complete water conservation neglects a small loss of entropy from hydrometeors that normally fall out of the parcel. Reversibility of the transformations does not strictly hold in our model since condensation and evaporation may happen in non-equilibrium conditions (i.e. $S_l \neq 1$, $S_i \neq 1$, which is unavoidable when mixed phase transformations are considered). However, the tendency in θ_{il} arising from irreversibility has small effect on the temperature profile, as shown by Bryan and Fritsch (2004), and we therefore neglect it.

Conservation of ice-liquid water potential temperature yields:

$$\frac{d\theta_{il}}{dz} = 0, \quad (4)$$

with θ_{il} given by:

$$\begin{aligned} \theta_{il} = & T \left(\frac{p_0}{p} \right)^{\chi} \left(1 - \frac{r_l + r_l^{(p)} + r_i + r_i^{(p)}}{e + r_t} \right)^{\chi} \left(1 - \frac{r_l + r_l^{(p)} + r_i + r_i^{(p)}}{r_t} \right)^{-\theta} \\ & \times \exp \left[\frac{-L_v (r_l + r_l^{(p)}) - L_s (r_i + r_i^{(p)})}{(c_p + c_{pv} r_t) T} \right. \\ & \left. + \frac{R_v^*}{c_p + c_{pv} r_t} \left((r_l + r_l^{(p)}) \ln S_l + (r_i + r_i^{(p)}) \ln S_i \right) \right], \quad (5) \end{aligned}$$

Vapour isotopic composition in updrafts

M. Bolot et al.

Title Page

Abstract

Introduction

Conclusions

References

Tables

Figures

◀

▶

◀

▶

Back

Close

Full Screen / Esc

Printer-friendly Version

Interactive Discussion



with

$$\chi = \frac{R^* + R_v^* r_t}{c_p + c_{pv} r_t},$$

$$\vartheta = \frac{R_v^* r_t}{c_p + c_{pv} r_t}.$$

5 3.2.2 Vapour pressure adjustment to saturation

At temperatures above 0°C, we assume that clouds are entirely liquid and vapour at saturation over liquid water, following previous studies (Warner, 1968; Korolev and Mazin, 2003) that exclude supersaturation over liquid reaching above a few percent. In the mixed-phase region between 0°C and -40°C, where both liquid water and ice can coexist, we assume that water vapour partial pressure adjusts instantaneously to some intermediate value e_{adj} between the saturated pressure over liquid water and the saturated pressure over ice. That is, vapour pressure is parameterized as a fixed linear combination of ice and liquid saturated pressures through a coefficient ζ such that $e_{\text{adj}} = e_{\text{sat}}^l \zeta + e_{\text{sat}}^i (1 - \zeta)$. Stipulating that $\zeta \leq 1$ ensures that vapour pressure in the mixed phase zone is supersaturated over ice and subsaturated over liquid; choosing $\zeta = 1$ would yield liquid water saturation ($e_{\text{sat}} = e_{\text{sat}}^l$). Once temperatures cool below -40°C, the cloud is assumed to be entirely glaciated and the degree of supersaturation assigned over ice is fixed from that point on. (Table 1 relates this final supersaturation to the parameter ζ).

Vapour isotopic composition in updrafts

M. Bolot et al.

Title Page

Abstract

Introduction

Conclusions

References

Tables

Figures

◀

▶

◀

▶

Back

Close

Full Screen / Esc

Printer-friendly Version

Interactive Discussion



Water vapour mixing ratio is thus parameterized as $r_v = r_{\text{adj}}$ with:

$$r_{\text{adj}} = e \frac{e_{\text{adj}}}{p - e_{\text{adj}}},$$

$$e_{\text{adj}} [T > 0^\circ\text{C}] = e_{\text{sat}}^l,$$

$$e_{\text{adj}} [-40^\circ\text{C} < T < 0^\circ\text{C}] = \left[e_{\text{sat}}^l [T] \zeta + e_{\text{sat}}^i [T] (1 - \zeta) \right], \quad (6)$$

$$e_{\text{adj}} [T < -40^\circ\text{C}] = \left[1 - \zeta + \frac{e_{\text{sat}}^l [T = -40^\circ\text{C}]}{e_{\text{sat}}^i [T = -40^\circ\text{C}]} \zeta \right] e_{\text{sat}}^i [T].$$

In convective clouds, the vapour available for deposition of condensate (either liquid or ice) comes either from adiabatic cooling of moisture in updrafts or from the re-evaporation of liquid water in the Wegener-Bergeron-Findeisen process (see next subsection). The only vapour sink is diffusional growth of the condensed phases. Vapour in an updraft will be supersaturated, but the degree of saturation will depend on the speed of the updraft, on the number concentration of liquid and ice particles, and on the mean equivalent radius of liquid and ice particles (Korolev and Mazin, 2003). The situation is further complicated by the effects of transients in phase relaxation (Korolev and Mazin, 2003), especially at lower temperatures. Accurately modelling vapour saturation in convective clouds is therefore difficult. One component of the interest in water isotopologues lies in the possible ability of isotopic measurements to provide insights into in-cloud supersaturation levels. The model parametrization here is somewhat arbitrary but is suitable for investigating this issue.

3.2.3 Droplet and cloud ice mass balance

The change in the amount of liquid or ice held by a parcel as it rises can be broken into three components: diffusional growth of condensates as ambient saturation changes, conversion of condensates from one phase (liquid, ice) to another, and auto-conversion

Vapour isotopic composition in updrafts

M. Bolot et al.

Title Page

Abstract

Introduction

Conclusions

References

Tables

Figures

◀

▶

◀

▶

Back

Close

Full Screen / Esc

Printer-friendly Version

Interactive Discussion



of condensates to deactivated/precipitated species. Even the simplest isotopic model must represent all three effects.

As an air parcel is lifted adiabatically, condensed phases take up vapour to maintain the adjusted vapour mixing ratio specified in Eq. (6). In the warm, liquid-only domain ($T > 0^\circ\text{C}$), growth occurs as liquid; in the glaciated domain ($T < -40^\circ\text{C}$) it occurs as ice; and only in the intermediate mixed-phase domain may it occur as either. We will however rule out liquid growth below 0°C , as we rule out vapour pressure above liquid saturation in the mixed phase domain.

We represent growth in all three zones by a single set of equations, turning time derivatives into vertical derivatives, based on the stationarity assumption:

$$\left. \frac{dr_i}{dz} \right|_{\text{ajs}} = -\xi_i \frac{dr_{\text{adj}}}{dz}, \quad (7)$$

$$\left. \frac{dr_l}{dz} \right|_{\text{ajs}} = -(1 - \xi_i) \frac{dr_{\text{adj}}}{dz}. \quad (8)$$

where ξ_i is the fraction of condensate growth resulting in ice deposition. ξ_i is set to 0 in the liquid domain, 1 in the glaciated domain and, as explained above, is also set to 1 in the mixed phase domain.

In the mixed-phased zone, liquid cloud droplets can be converted to ice by two processes: either by direct freezing of droplets (presumably heterogeneous at $T < -35^\circ\text{C}$, and homogeneous otherwise) or by the “Wegener-Bergeron-Findeisen” (WBF) process (Wegener, 1911; Bergeron, 1935; Korolev, 2007) in which cloud droplets evaporate, providing an extra source of water vapour that then deposits as ice on growing crystals. We will throughout this derivation simply assume that an arbitrary fraction b of liquid water is converted to ice through the WBF process vs. droplet freezing. As freezing does not involve diffusive exchanges of isotopologues with vapour, unlike WBF, the two processes have very different isotopic signatures.

Vapour isotopic composition in updrafts

M. Bolot et al.

[Title Page](#)[Abstract](#)[Introduction](#)[Conclusions](#)[References](#)[Tables](#)[Figures](#)[◀](#)[▶](#)[◀](#)[▶](#)[Back](#)[Close](#)[Full Screen / Esc](#)[Printer-friendly Version](#)[Interactive Discussion](#)

Regardless of the relative importance of the WBF process, though, the combination of both processes is parameterized as a single conversion rate of liquid water to ice φ :

$$\left. \frac{dr_i}{dz} \right|_{\text{cli}} = \left. \frac{dr_i}{dz} \right|_{\text{frz}} + \left. \frac{dr_i}{dz} \right|_{\text{wbf}} = \varphi(T) r_i, \quad (9)$$

$$\left. \frac{dr_i}{dz} \right|_{\text{cli}} = \left. \frac{dr_i}{dz} \right|_{\text{frz}} + \left. \frac{dr_i}{dz} \right|_{\text{wbf}} = -\varphi(T) r_i. \quad (10)$$

The temperature dependence of the conversion rate φ is chosen to ensure zero conversion at $T = 0^\circ\text{C}$ and maximum conversion at $T = -40^\circ\text{C}$:

$$\varphi(T) = \frac{1}{50} \left(\frac{273.15 - T}{40} \right)^\gamma, \quad (11)$$

where T is in Kelvin. The parameter γ controls the rate of glaciation of the cloud. Higher γ produces lower glaciation rates which delay cloud glaciation and allow significant amounts of supercooled liquid to persist to higher altitudes. For the sake of illustration, let us assume a linear variation of temperature with altitude in the mixed phase region. The falloff in liquid water with altitude in the mixed-phase region, under the sole action of liquid to ice conversion (no auto-conversion), is derived by integrating Eq. (10) over the range of altitude between 0°C and -40°C , and yields:

$$\ln \left(\frac{r_i}{r_i[0^\circ\text{C}]} \right) \sim \frac{z[0^\circ\text{C}] - z[-40^\circ\text{C}]}{50(\gamma + 1)} \left(\frac{z[0^\circ\text{C}] - z}{z[0^\circ\text{C}] - z[-40^\circ\text{C}]} \right)^{\gamma+1}. \quad (12)$$

The altitude above which r_i drops below some threshold clearly increases with γ . By convention, we define the glaciation temperature T_g and glaciation altitude z_g as the location where $r_i = 10^{-6} \text{ kg kg}^{-1}$ is reached. Glaciation altitude depends mainly on γ , but depends slightly on the conversion of droplets to deactivated/precipitated species (discussed below) and very slightly on the supersaturation. This dependency is illustrated in Table 1.

Vapour isotopic composition in updrafts

M. Bolot et al.

Title Page

Abstract

Introduction

Conclusions

References

Tables

Figures

◀

▶

◀

▶

Back

Close

Full Screen / Esc

Printer-friendly Version

Interactive Discussion



We represent the auto-conversion of condensates to deactivated/precipitated species (the $(l^{(p)})$ and $(i^{(p)})$ water classes introduced in Sect. 3.1) as a constant fractional loss of mass from the activated liquid (l) and ice (i) water classes:

$$\left. \frac{dr_i}{dz} \right|_{\text{acv}} = -C_i r_i, \quad (13)$$

$$\left. \frac{dr_l}{dz} \right|_{\text{acv}} = -C_l r_l, \quad (14)$$

$$\left. \frac{dr_i^{(p)}}{dz} \right|_{\text{acv}} = C_i r_i, \quad (15)$$

$$\left. \frac{dr_l^{(p)}}{dz} \right|_{\text{acv}} = C_l r_l. \quad (16)$$

where C_l and C_i are fractional auto-conversion coefficients for liquid water and ice.

Combining all these effects, we can write expressions for the vertical variation of the liquid water and ice mixing ratios:

$$\frac{dr_i}{dz} = -\xi_i \frac{dr_{\text{adj}}}{dz} - C_i r_i + \varphi(T) r_l, \quad (17)$$

$$\frac{dr_l}{dz} = -(1 - \xi_l) \frac{dr_{\text{adj}}}{dz} - C_l r_l - \varphi(T) r_i, \quad (18)$$

along with Eqs. (15)–(16) for the deactivated/precipitated components.

The full model of light water transformations in the convective plume then consists of Eq. (2) (water mass balance); Eqs. (15)–(18) (tendencies for the (l), (i), $(l^{(p)})$, and $(i^{(p)})$ water classes); Eqs. (4) and (5) (thermodynamics); and Eq. (6) (vapour saturation assignment).

Vapour isotopic composition in updrafts

M. Bolot et al.

Title Page

Abstract

Introduction

Conclusions

References

Tables

Figures

◀

▶

◀

▶

Back

Close

Full Screen / Esc

Printer-friendly Version

Interactive Discussion



3.2.4 Model solving

The full model has 6 z -dependent variables, the temperature T and the light water mixing ratios $\mathbf{r} = (r_v, r_l, r_i, r_l^{(p)}, r_i^{(p)})$. The control parameters (ζ, γ, C_l, C_i) are fixed. Boundary conditions must be provided at cloud base. At cloud base, water vapour is assumed to be saturated, with all condensate water classes set to zero and the ice-liquid potential temperature set at a value $\theta_{il} = \theta_{il0}$, which is then preserved aloft within the convective plume. The stratification in the environment of the cloud is assumed to be hydrostatic.

The set of equations of the model can be reduced to the mixing ratios equations:

$$\frac{d\mathbf{r}}{dz} = \mathbf{F} \left(\mathbf{r}, \frac{dT}{dz}, T, \rho \right), \quad (19)$$

and the thermodynamic equation:

$$0 = \frac{d\theta_{il}}{dz} \left(T, \frac{dT}{dz}, \mathbf{r}, \frac{d\mathbf{r}}{dz}, \rho \right). \quad (20)$$

After replacement of $d\mathbf{r}/dz$ using Eq. (19), Eq. (20) is turned into an implicit equation for dT/dz which is solved iteratively after discretization. This solution is then readily used to make a step of T in the vertical and to make a step for the water classes mixing ratios \mathbf{r} in Eq. (19).

3.3 Vapour isotopic composition

The tendency on R_v may be derived from the conservation of heavy isotopologues:

$$\frac{d}{dz} \left(r'_v + r'_l + r'_i + r'_l^{(p)} + r'_i^{(p)} \right) = 0 \quad (21)$$

Vapour isotopic composition in updrafts

M. Bolot et al.

Title Page

Abstract

Introduction

Conclusions

References

Tables

Figures

◀

▶

◀

▶

Back

Close

Full Screen / Esc

Printer-friendly Version

Interactive Discussion



Expanding the terms of this equation into relevant physical processes yields five master equations:

$$\frac{dr'_v}{dz} = r_v \frac{dR_v}{dz} + R_v \frac{dr_v}{dz}, \quad (22)$$

$$\frac{dr'_l}{dz} = r_l \frac{dR_l}{dz} + R_l \left(\left. \frac{dr_l}{dz} \right|_{ajs} + \left. \frac{dr_l}{dz} \right|_{wbf} + \left. \frac{dr_l}{dz} \right|_{frz} + \left. \frac{dr_l}{dz} \right|_{acv} \right), \quad (23)$$

$$\frac{dr'_i}{dz} = R_i^{(s)} \left(\left. \frac{dr_i}{dz} \right|_{ajs} + \left. \frac{dr_i}{dz} \right|_{wbf} \right) + R_l \left. \frac{dr_i}{dz} \right|_{frz} + R_i^{(p)} \left. \frac{dr_i}{dz} \right|_{acv}, \quad (24)$$

$$\left. \frac{dr'_l{}^{(p)}}{dz} \right|_{acv} = R_l \left. \frac{dr_l^{(p)}}{dz} \right|_{acv}, \quad (25)$$

$$\left. \frac{dr'_i{}^{(p)}}{dz} \right|_{acv} = R_i^{(p)} \left. \frac{dr_i^{(p)}}{dz} \right|_{acv}, \quad (26)$$

that we now discuss in greater detail.

The first two equations (22) and (23) simply reflect the definition of the isotopic ratios for vapour and liquid: $r'_v = r_v R_v$ and $r'_l = r_l R_l$. The liquid mixing ratio R_l here is predicated on an assumption that all cloud water has homogeneous composition $R_l = \alpha_{kl}^{(eq)} R_v$. If droplets froze slowly relative to isotopic exchange timescales between liquid and vapour, we would need an additional term describing the extraction of further heavy water from the vapour phase as an ice germ grows within the droplet. However, droplet freezing can robustly be assumed to be fast relative to exchanges timescales (see Appendix D).

The third equation, Eq. (24), describes the tendency of heavy isotopologues in ice. The isotopic ratio at ice surface, $R_i^{(s)}$, appears in the right hand side for the two processes that involve diffusional growth of ice crystals (growth following adjustment of

Vapour isotopic composition in updrafts

M. Bolot et al.

Title Page

Abstract

Introduction

Conclusions

References

Tables

Figures

◀

▶

◀

▶

Back

Close

Full Screen / Esc

Printer-friendly Version

Interactive Discussion



Vapour isotopic composition in updrafts

M. Bolot et al.

Title Page

Abstract

Introduction

Conclusions

References

Tables

Figures

◀

▶

◀

▶

Back

Close

Full Screen / Esc

Printer-friendly Version

Interactive Discussion



vapour saturation and the WBF process). These two processes produce kinetic fractionation between vapour and ice surface ($R_i^{(s)} = \alpha_{ki}R_v$). The two remaining terms describe the source from droplet freezing and the sink from auto-conversion. Freezing has to be represented separately from the WBF process because it preserves the isotopic composition of the freezing droplet, whereas transition through the vapour phase in the WBF process involves fractionation.

The final two equations, Eqs. (25) and (26), describe the auto-conversion of liquid water and ice to deactivated/precipitated species. Deactivated liquid droplets carry the isotopic composition of the cloud water class at the time of deactivation. Deactivation of liquid droplets affect vapour composition by modifying the size of the liquid water reservoir that exchanges with vapour. In contrast, precipitation of ice in Eq. (24) has no effect on the water vapour isotopic composition, since ice did not exchange with vapour in the first place. Therefore the net isotopic content of precipitating ice $R_i^{(p)}$, which depends on the ice crystal size distribution and individual crystal isotopic composition, may take any value without affecting our results as seen below.

The isotopic composition of water vapour R_v can then be determined analytically by expanding Eq. (21) using Eqs. (22)–(26) and using the expressions for light water microphysical tendencies derived in Sect. 3.2.3. We neglect fractional changes in α_{ki} , compared to that in R_v , implying that $dR_i/dz \sim \alpha_{ki}dR_v/dz$. Carrying through the calculations yields the following expression:

$$\frac{d \ln R_v}{dz} = \left[(\xi_i \alpha_{ki} + (1 - \xi_i) \alpha_{kl} - 1) \frac{dr_v}{dz} - b \varphi(T) r_1 (\alpha_{ki} - \alpha_{kl}) \right] \times \frac{1}{r_v + \alpha_{kl} r_1}, \quad (27)$$

The parameter b is the fraction of liquid to ice conversion occurring via the WBF process (see Sect. 3.2.3) as opposed to via direct freezing. It is convenient to define a WBF parameter η that measures the ratio between the amount of water vapour deposited as ice that results from droplet evaporation to that resulting from decreasing

vapour pressure due to adiabatic cooling of the parcel:

$$\eta = \frac{b\varphi(T)r_1}{-dr_v/dz}, \quad (28)$$

Eq. (27) then reads:

$$d \ln R_v/dz = [\Lambda(T, S_i, \eta) - 1] \frac{dr_v/dz}{r_v + \alpha_{kl}r_1}, \quad (29)$$

5 where

$$\Lambda(T, S_i, \eta) = \xi_i \alpha_{ki} + (1 - \xi_i) \alpha_{kl} + \eta(\alpha_{ki} - \alpha_{kl}) \quad (30)$$

is a generalised fractionation factor that depends on temperature, cloud saturation and on the intensity of the WBF process.

10 Equation (29) is equivalent to Eq. (18) of Federer et al. (1982) if we drop entrainment (i.e. set $\mu = 0$) and diffusive isotopic exchange with rain (i.e. set $P'_{vr} = 0$) in their representation, and notice that $(1 - \xi_i - \eta)dr_v/dz = P_{vc}$ and $(\xi_i + \eta)dr_v/dz = P_{vi}$, where P_{vc} and P_{vi} are, respectively, their production term for cloud water and cloud ice.

15 Equation (29) offers many deep insights on inspection. The generalised fractionation factor Λ contains only the processes involving diffusive exchanges of isotopologues with vapour and excludes freezing and auto-conversion processes. The term $\xi_i \alpha_{ki} + (1 - \xi_i) \alpha_{kl} - 1$ in Eq. (30) corresponds to the net growth of droplets and ice crystals driven by adiabatic cooling, while $\eta(\alpha_{ki} - \alpha_{kl})$ corresponds to the isotopic changes induced by the WBF process. The former term is always larger than 1 and leads to a depletion of heavy isotopologues in the vapour phase. In other words, net growth of
20 droplets or ice crystals following parcel cooling results in the well-known progressive distillation of heavy isotopologues out of the vapour phase. The WBF term, on the other hand, can be of either sign depending on the magnitude of liquid-ice disequilibrium (discussed in length in Sect. 4.3). If kinetic effects are strong, the fractionation factor over

liquid may actually exceed that over ice: $\alpha_{kl} > \alpha_{ki}$. In these conditions, if a significant fraction of droplet freezing occurs via the WBF, then the WBF term may outweigh the net distillation term and actually lead to local isotopic enrichment of water vapour.

3.4 Impact of glaciation on isotopic distillation

The presence of liquid water reduces distillation over the case where liquid water is absent: cloud droplets retained within the parcel buffer vapour isotopic composition by exchanging isotopically with the vapour. This effect is represented by the component $\alpha_{kl}r_1$ in the denominator of the unbracketed term in Eq. (29). In the case where all condensates are removed from the parcel and no liquid water is retained ($r_1 = 0$), buffering vanishes and the overall expression for change in vapour isotopic composition reduces to a pure Rayleigh distillation process (Rayleigh and Ramsay, 1895; Dansgaard, 1964) with a modified fractionation factor (Λ). Maximum buffering from re-equilibration between vapour and liquid occurs when r_1 is maximum, i.e. when precipitation efficiency is zero and all condensates are retained and can exchange with water vapour. This condition is termed the adiabatic scenario by Jouzel et al. (1975). The loss of liquid water on glaciation results in a well-known transition between liquid and ice regimes during parcel ascent (Federer et al., 1982; Moyer et al., 1996).

For illustrative purposes, we obtain an approximate solution in the ice and liquid regime by setting Λ constant. This assumption is in most regions reasonable, since r_v may vary by four orders of magnitude during the ascent of a deep convective system to the tropopause, but $\Lambda - 1$ varies at most by a factor of 5. The approximate solution in the warm, liquid-only region under the adiabatic assumption is found by replacing Λ (and α_{kl}) by a fixed fractionation factor Λ_0 and assuming $r_v + r_1$ to be constant. Equation (29) can then be integrated to yield:

$$R_v = \frac{R_{v0}r_{v0}}{\Lambda_0 r_{v0} - (\Lambda_0 - 1)r_v}, \quad (31)$$

where R_{v0} and r_{v0} are cloud base values of R_v and r_v .

22475

Vapour isotopic composition in updrafts

M. Bolot et al.

Title Page

Abstract

Introduction

Conclusions

References

Tables

Figures

◀

▶

◀

▶

Back

Close

Full Screen / Esc

Printer-friendly Version

Interactive Discussion



The approximate solution in the ice-only regime is found by setting r_i to zero to yield the expression for Rayleigh distillation:

$$R_v = R_{v1} \left(\frac{r_v}{r_{v1}} \right)^{\Lambda_0 - 1}, \quad (32)$$

where (R_{v1}, r_{v1}) is a reference point on the Rayleigh curve. These “adiabatic” and “Rayleigh” solutions are shown in Fig. 4 along with the full integrated solution of Eq. (29). The behaviour of the full solution is well reproduced other than in the coldest uppermost troposphere (where α_i departs significantly from Λ_0) and of course in the transition region between regimes.

As would be expected, the two approximate solutions yield very different asymptotic values in the limit where all vapour is removed from the air parcel ($r_v \rightarrow 0$). In the Rayleigh regime, loss of all vapour corresponds to complete distillation of heavy isotopologues out of the vapour phase: $R_v \rightarrow 0$ when $r_v \rightarrow 0$. In the adiabatic regime, R_v saturates at a finite value R_{v0}/Λ_0 when liquid water dominates total water. This value corresponds to the state of vapour in isotopic equilibrium with liquid water when the latter inherits the surface isotopic ratio of water vapour.

In the real world, rainout in the warm phase will limit the buffering effect provided by liquid water. In this case the adiabatic solution would overestimate the heavy isotopologue content during the initial stage of the ascent. Nevertheless, the presence of liquid water is a powerful factor in isotopic evolution. In the mixed phase region, the location of the transition to the Rayleigh regime is governed by any inhibition of glaciation that allows supercooled water to persist and remain a significant fraction of total water.

4 Sensitivity of vapour isotopic composition to cloud physics

In this section, we use the framework developed above to explore the sensitivity of the isotopic composition of water vapour to cloud processes and parameters: supersaturation, retention of liquid water, and the nature of glaciation. In each set of experiments

Vapour isotopic composition in updrafts

M. Bolot et al.

Title Page

Abstract

Introduction

Conclusions

References

Tables

Figures



Back

Close

Full Screen / Esc

Printer-friendly Version

Interactive Discussion



we vary a single parameter and keep others fixed. Isotopic profiles are determined by integrating Eq. (29) from surface to tropopause along the trajectory of a rising air parcel. A similar approach was followed by Federer et al. (1982) and Moyer et al. (1996). However, to our knowledge no further extensive study of sensitivity of isotopic profiles to microphysics in convective systems has been conducted.

The reference scenario (i.e. we vary one parameter at a time around this reference) from which the sensitivity studies are performed assumes that:

- there is no auto-conversion to deactivated/precipitated species (i.e. $C_1 = 0$ and $C_i = 0$)
- the WBF process plays no role ($b = \eta = 0$)
- glaciation occurs between temperatures of -26°C and -30.5°C (the glaciation parameter is $\gamma = 3.5$, see table 1)
- saturation is maximum with respect to ice and saturates at 147 % for temperatures below -40°C (i.e. the saturation parameter is $\zeta = 1$)

We stress again that the parameter space explored is bounded by the assumptions that water vapour is never subsaturated with respect to ice or liquid water and never supersaturated over liquid water. Consequently liquid water is not allowed to grow below 0°C .

The model integration assumes conditions typical of the tropics. We take a cloud base at 1050 m and take the temperature profile below this altitude from a multi-annual average of the ERA-Interim reanalysis (Dee et al., 2011) within the 20°S – 20°N latitude band. The isotopic ratios are initialised at cloud base with ratios typical of the marine boundary layer for a relative humidity of 95 % and under quiescent weather conditions: $\delta\text{D} = -70\text{‰}$ and $\delta^{18}\text{O} = -10\text{‰}$ (Craig and Gordon, 1965; Lawrence et al., 2004). All other microphysical constants and parameters are given in the Appendix.

Vapour isotopic composition in updrafts

M. Bolot et al.

Title Page

Abstract

Introduction

Conclusions

References

Tables

Figures

◀

▶

◀

▶

Back

Close

Full Screen / Esc

Printer-friendly Version

Interactive Discussion



4.1 Sensitivity to vapour saturation

Although we do not consider supersaturation over liquid in the liquid-only cloud regime, supersaturation over ice in the mixed-phase and ice-only regime can have strong isotopic effects (Dansgaard, 1964; Jouzel and Merlivat, 1984; Moyer et al., 1996). As S_i increases, the effective fractionation factor will decrease at any temperature, for both HDO/H₂O and H₂¹⁸O/H₂O, though the effects are stronger for H₂¹⁸O/H₂O. (See Sect. 2.3 for discussion of kinetic fractionation).

We first explore the effects of varying supersaturation in the absence of the WB process ($\eta = 0$). In our model, the specification of a constant saturation parameter ζ by definition produces a gradual increase in supersaturation over ice as the cloud glaciates. The effect of that growing supersaturation on $-(\Lambda - 1) = 1 - \alpha_{ki}$ is shown in Figs. 5a and 6a, where choices of ζ from 0 to 1 produce final supersaturation over ice from 100 % to 150 %. Within this range of S_i , at -40°C , $1 - \alpha_{ki}$ varies for HDO/H₂O by a factor of 1.5, from -0.23 to -0.15 (Fig. 5a), and that for H₂¹⁸O/H₂O by a factor of 3, from -0.03 to -0.01 (Note from Eq. 29 that $1 - \alpha_{ki}$ is the relevant metric for comparison of isotopic effects rather than the effective fractionation factor α_{ki}). At lower temperatures, relative variations of $1 - \alpha_{ki}$ with saturation stay of the same order.

The resulting effects on isotopic profiles are shown in panels (a) and (d) of Fig. 7. While isotopic changes in the glaciation region itself are small, supersaturations persist during the remaining ascent to the tropopause, and progressive distillation as water vapour deposits to ice means that supersaturation can produce substantial isotopic effects: supersaturations of 100–150 % (ζ of 0–1) produce isotopic profiles differing at most by $\sim 50\%$ for δD and $\sim 150\%$ for $\delta^{18}\text{O}$. (The curves in panel a actually converge at the coldest temperatures, not because of any saturation effect but because the large mass ratio D/H produces such strong fractionations that by very cold temperatures, deuterium is fully stripped out of the vapour phase, that is $\delta\text{D} \rightarrow -1000\%$, and the metric δD loses sensitivity to saturation).

Vapour isotopic composition in updrafts

M. Bolot et al.

Title Page

Abstract

Introduction

Conclusions

References

Tables

Figures

◀

▶

◀

▶

Back

Close

Full Screen / Esc

Printer-friendly Version

Interactive Discussion



Vapour isotopic composition in updrafts

M. Bolot et al.

Title Page

Abstract

Introduction

Conclusions

References

Tables

Figures

◀

▶

◀

▶

Back

Close

Full Screen / Esc

Printer-friendly Version

Interactive Discussion



The sensitivity of water isotopologues to supersaturation means that if numerical convective schemes are to realistically reproduce isotopic profiles they must involve a careful parameterization of in-cloud supersaturation. Simplified parameterizations that depend only on temperature may not be appropriate in convective models. The appropriate physics for supersaturation in convective clouds involves a balance between the adiabatic cooling rate of moisture and the rate of vapour uptake due to growth of condensed phase (Squires, 1952; Twomey, 1959; Korolev and Mazin, 2003). Higher updraft speeds, lower concentration of ice particles or smaller crystals will result in higher supersaturations over ice, which limits isotopic fractionation, especially for ^{18}O .

Theory suggest that supersaturation in convective clouds can be highly variable, and reach values as high as saturation over liquid. The conditions of sustained liquid saturation in a convective updraft can be derived within the theoretical framework developed by Korolev and Mazin (2003). For an ice number concentration of 5 cm^{-3} and a mean ice equivalent radius of $20\text{ }\mu\text{m}$ (which are in the range of observations for maritime convection) (Lawson et al., 2010; Stith et al., 2002)), steady-state liquid saturation at $-20\text{ }^{\circ}\text{C}$ (i.e. 22% supersaturation over ice) may be sustained in a vertical stream of at least 16 ms^{-1} . If ice number concentration falls to lower values, liquid saturation is even more readily sustained. However, many modelling studies, including at mesoscale (Hoffmann et al., 1998; Schmidt et al., 2007; Lee et al., 2007; Yoshimura et al., 2008; Tindall et al., 2009; Risi et al., 2010; Kurita et al., 2011), use a parameterization of ice supersaturation of the form $S_i = 1 - \lambda T [^{\circ}\text{C}]$ (initially derived by Jouzel and Merlivat, 1984 to represent supersaturation in inversion layers over Greenland and Antarctica). These parameterizations limit supersaturation over ice at $-20\text{ }^{\circ}\text{C}$ to 6–10%, for the range of choices in λ (between $0.003\text{ }^{\circ}\text{C}^{-1}$ and $0.005\text{ }^{\circ}\text{C}^{-1}$ according to Risi et al., 2012), less than half that estimated above for vigorous convection. The sensitivity of isotopic compositions to supersaturation means that this discrepancy is significant for models that track the isotopic composition of water vapour, and should be a focus of future study. (See further discussion in Sect. 5.)

4.2 Sensitivity to (isotopically active) liquid water content

Liquid water content in clouds is affected by entrainment rates, updraft velocities, precipitation efficiencies and the relative dominance of warm rain versus ice processes (Cotton et al., 2011, chap. 8.12). The amount of supercooled water persisting in the “mixed-phase zone” between 0 and -40°C is also quite variable. Near-complete retention of liquid water has been observed: for instance, Rosenfeld and Woodley (2000) measured a near-adiabatic liquid water content of 1.8 gm^{-3} down to -37.5°C in a case of vigorous continental convection over Texas. The other extreme case of full glaciation at much warmer temperatures is also possible: Stith et al. (2004) found no liquid water at temperatures colder than -17°C in cases of maritime convection over Kwajalein. The isotopic effects that arise from these variations in the size of the actively exchanging liquid water reservoir are strong. For instance, in the case of continental convection just mentioned, a conservative assumption of 20 ms^{-1} for the updraught velocity and reported values of median volume diameter of supercooled droplets yields a median volume isotopic adjustment length scale of 14 m at -10°C , 39 m at -20°C and 200 m at -35°C . (See also Sect. 2.3.) This increase suggests that a significant part of liquid water may not fully equilibrate with vapour at temperatures lower than -20°C , at least during the active stage of convection. In other words, the combined variability in the liquid water content and in the fraction of actively exchanging droplets significantly impacts water vapour isotopic composition within convective systems.

In our model, the vertical profile of active liquid water is primarily governed by two parameters that control auto-conversion processes and the ability of supercooled droplets to survive at negative temperatures: C_1 , the auto-conversion coefficient and γ , which controls the conversion of liquid to ice and effectively sets the glaciation altitude.

Figure 7 (panels b and e) shows that vapour isotopic composition is sensitive to the altitude of glaciation. Changing the glaciation altitude (via γ) with other parameters held fixed changes the level of transition from the adiabatic to the Rayleigh isotopic regimes. Trajectories where the cloud glaciates fully at lower altitudes (higher temperatures)

Vapour isotopic composition in updrafts

M. Bolot et al.

Title Page

Abstract

Introduction

Conclusions

References

Tables

Figures

◀

▶

◀

▶

Back

Close

Full Screen / Esc

Printer-friendly Version

Interactive Discussion



produce more depleted vapour isotopic compositions in the middle and upper troposphere, since the strong Rayleigh fractionation over ice begins earlier. If supercooled water is retained to higher altitudes (lower temperature), vapour isotopic composition is relatively enhanced. The isotopic differences at some altitudes may be larger than 100‰ for δD .

The sensitivity of isotopic profiles to auto-conversion efficiency is also strong (panels c and f of Fig. 7). In this case, we vary C_1 from 0 (adiabatic active water content) to 0.5 km^{-1} . At the highest value of C_1 , active liquid water content at 0°C level is reduced to 31 % of its adiabatic value. When $C_1 = 0$, the transition between the adiabatic regime in which vapour exchanges with liquid cloud water to the Rayleigh regime is sharp. As active liquid water content decreases, its buffering effect is reduced and the transition between regimes becomes less sharp. In the limit of full auto-conversion, $r_1 = 0$ and isotopic evolution throughout cloud ascent occurs by pure Rayleigh distillation.

Moyer et al. (1996) described a similar dependency of cloud vapour isotopic composition to condensate retention, under the assumption that all droplets actively reequilibrate, and showed the limiting cases of no precipitation and full condensate retention. Federer et al. (1982) pointed out that their microphysical model exhibits an adiabatic behaviour when raindrops are excluded from consideration as a result of assuming a continental droplet spectrum. They also assumed that droplets are always in isotopic equilibrium with vapour. Our model results (Fig. 7) agree with previous work in showing that the isotopic consequences of retention of liquid water are strongest in the mid-troposphere. Once glaciation is complete, isotopic differences due to liquid water content are gradually eroded by continued distillation.

4.3 Droplet evaporation in the mixed phase region (WBF)

In subsections 4.1 and 4.2, glaciation was assumed to occur by freezing of liquid droplets, so that the phase change itself does not produce fractionation. If glaciation proceeds instead via the WBF process (liquid-vapour-ice), as previously shown, it produces fractionation. We explore these isotopic effects in our model by varying the

Vapour isotopic composition in updrafts

M. Bolot et al.

Title Page

Abstract

Introduction

Conclusions

References

Tables

Figures

⏪

⏩

◀

▶

Back

Close

Full Screen / Esc

Printer-friendly Version

Interactive Discussion



parameter b , which governs the fraction of glaciation that occurs via WBF, from $b = 0$ (no WBF) to $b = 1$ (all glaciation by WBF). The glaciation parameter γ is set to a high value, 9, to move final glaciation to a high altitude, since isotopic effects of the WBF process are most obvious at low temperatures.

As seen in Fig. 8, the main isotopic effect produced by the WBF is an enhancement in heavy isotopologues of water vapour that occurs in the glaciation region. The enhancement occurs because effective fractionation over liquid becomes larger than effective fractionation over ice at small temperature, as was recognized by Ciais and Jouzel (1994) and Moyer et al. (1996). This effect is illustrated in Figs. 5b and 6b. The reason for this reversal is that as temperature decreases, kinetic isotopic effects decrease α_{ki} and increase α_{kl} , as a result of growing liquid-ice disequilibrium, until they cross. At this point, transferring water from liquid to vapour and then re-condensing it as ice produces enrichment of vapour, since freshly deposited ice is isotopically lighter than the supercooled droplets. However, net ice deposition following adiabatic cooling, corresponding to the term $1 - \alpha_{ki}$ in Λ , always results in a depletion of vapour isotopic composition. The balance between these two counteracting processes produces the isotopic profiles seen in Fig. 8. The section of net isotopic enhancement occurs only at cold temperatures, when droplet evaporation can supply enough vapour to outweigh the effects of adiabatic moisture cooling. This enhancement scales with the importance of the WBF process in glaciation (i.e. b).

While Fig. 8 shows isotopic profiles for only a single assumption of glaciation altitude ($\gamma = 9$), the occurrence and location of the isotopic enhancement in different glaciation conditions can be inferred from examining the generalised fractionation factor Λ . Figures 5c and 6c show $-(\Lambda - 1) = 1 - \alpha_{ki} - \eta(\alpha_{kl} - \alpha_{ki})$, combining both WBF and net ice deposition, over the entire mixed phase region for a range of the WBF parameter η . As discussed previously, η measures the ratio of the source of vapour from droplets evaporation to that from net adiabatic cooling of moisture (it thus measures the magnitude of WBF). Variations of η with cloud temperature are superimposed on the same panel, for rising parcels with several values of the glaciation parameter γ (b is fixed to

Vapour isotopic composition in updrafts

M. Bolot et al.

Title Page

Abstract

Introduction

Conclusions

References

Tables

Figures

◀

▶

◀

▶

Back

Close

Full Screen / Esc

Printer-friendly Version

Interactive Discussion



1 in those simulations). The values of η exhibit excursions which peak at temperatures somewhat warmer than the glaciation temperatures of the parcels and decreasing with increasing γ . This variation is due to enhanced conversion of liquid to ice near glaciation, while evaporation eventually tails off as liquid water becomes depleted. The generalised fractionation factor (or rather $-(\Lambda - 1)$ here) is then determined according to the temperature and the excursion in η along the trajectories of the parcels.

These results show that if glaciation is largely completed at low altitudes (warm temperatures), the WBF effect can only yield further isotopic depletion. Net enhancement of vapour isotopic composition via WBF occurs when $1 - \Lambda > 0$. This circumstance is reached only when sufficient liquid water is retained at cold temperatures ($\sim -30^\circ\text{C}$ or less). The isotopic effect of the WBF process therefore depends on the average level to which supercooled droplets have managed to survive conversion to ice. Note that WBF enhancement of isotopic composition occurs more readily for $\text{H}_2^{18}\text{O}/\text{H}_2\text{O}$ than for $\text{HDO}/\text{H}_2\text{O}$, with onset at warmer temperatures. This effect is not surprising, since the WBF is itself driven by the kinetic fractionation effects that are stronger for the system $\text{H}_2^{18}\text{O}/\text{H}_2\text{O}$ than for $\text{HDO}/\text{H}_2\text{O}$.

Conditions where the WBF effect is important could be produced when strong convection loses buoyancy and enters its dissipating stage. If a significant amount of supercooled droplets have survived to low temperatures during the preceding active stage, then ice will begin to grow at the expense of droplet evaporation in residual vapour-limited uplifts at temperatures above -40°C . These ice crystals eventually serve as seeds for stratiform precipitation. Theory predicts also that the WBF process is more efficient than heterogeneous freezing in transforming supercooled liquid to ice at these low temperatures (Orville and Kopp, 1977, Fig. 3). Thus, we speculate that the transition from convective to stratiform physics, in cases of strong convection, may produce an isotopic enhancement in the $\sim -30^\circ\text{C}$ to -40°C region, especially for ^{18}O .

Finally, note that models can only simulate WBF isotopic enhancement if they represent kinetic effects for both droplet evaporation and ice deposition within the mixed phase zone. If kinetic fractionation for droplet evaporation is neglected, as in Blossey

Vapour isotopic composition in updrafts

M. Bolot et al.

[Title Page](#)[Abstract](#)[Introduction](#)[Conclusions](#)[References](#)[Tables](#)[Figures](#)[◀](#)[▶](#)[◀](#)[▶](#)[Back](#)[Close](#)[Full Screen / Esc](#)[Printer-friendly Version](#)[Interactive Discussion](#)

et al. (2010), then enhancement is restricted to situations where all liquid water experiences conversion to ice immediately below the homogeneous freezing level. If kinetic effects are neglected for both droplet evaporation and ice deposition, as in Federer et al. (1982), then no enhancement is possible.

5 Deuterium oxygen-18 relationship

It is common in geochemistry, when multiple isotopologue systems are available, to utilize relationships between different isotopologues. These comparisons can both eliminate dependence on the concentration of the primary species and can elucidate subtle kinetic effects that affect isotopologues differently. With atmospheric water vapour, the very large change in concentration – four orders of magnitude from surface to tropopause – makes direct comparison of $\delta^{18}\text{O}$ and δD especially useful, and it has been used since the inception of isotopic measurements (e.g. Craig, 1961a; Dansgaard, 1964; Merlivat and Jouzel, 1979).

In our model, we can readily combine the separate distillation equations ($d\ln R_v/dz$) for $\text{HDO}/\text{H}_2\text{O}$ and $\text{H}_2^{18}\text{O}/\text{H}_2\text{O}$ (see Eq. 29) in order to eliminate the dependence on water vapour concentration. Combining these equations yields the local slope of δD vs. $\delta^{18}\text{O}$ in the vapour phase:

$$\frac{d\delta\text{D}}{d\delta^{18}\text{O}} = \underbrace{\left(\frac{R_0^{18\text{O}}}{R_0^{\text{D}}}\right)}_1 \underbrace{\left(\frac{R_v^{\text{D}}}{R_v^{18\text{O}}}\right)}_2 \underbrace{\left[1 + \frac{\alpha_{\text{kl}}^{18\text{O}} - \alpha_{\text{kl}}^{\text{D}}}{r_l + \alpha_{\text{kl}}^{\text{D}}}\right]}_3 \frac{\Lambda^{\text{D}} - 1}{\Lambda^{18\text{O}} - 1}, \quad (33)$$

where the superscript labels the isotopologue systems $\text{HDO}/\text{H}_2\text{O}$ and $\text{H}_2^{18}\text{O}/\text{H}_2\text{O}$.

Among the factors in the r.h.s of Eq. (33) that control the slope, the first two (term 1) are pure scaling terms. The third factor (term 2) contains the dependence upon liquid water content r_l . It is relatively invariant, being bounded between 1 and

Title Page

Abstract

Introduction

Conclusions

References

Tables

Figures

◀

▶

◀

▶

Back

Close

Full Screen / Esc

Printer-friendly Version

Interactive Discussion



$1 + 0.2(r_v/r_l + 1)^{-1}$ for temperature down to -40°C . Even in the most extreme case without liquid auto-conversion, water vapour would constitute at least 20 % of total water content in the lower troposphere ($r_v/r_l > 0.2$), so that this factor does not exceed 1.16. Thus, while liquid water re-equilibration with vapour has strong effects on isotopic ratios, it is relatively unimportant to the $\delta\text{D}-\delta^{18}\text{O}$ slope. The main factor controlling the slope (term 3) arises from the different tendencies of fractionation in $\text{HDO}/\text{H}_2\text{O}$ and $\text{H}_2^{18}\text{O}/\text{H}_2\text{O}$ for rising parcels and depends on the local thermodynamical and micro-physical conditions.

Figure 9 shows the vertical profile of the $\delta\text{D}-\delta^{18}\text{O}$ slope given by Eq. (33) bracketing its span with extreme choices for vapour saturation ($\zeta = 0$ and $\zeta = 1$, corresponding to 100 % and 147 % final saturation over ice, see Table 1) and glaciation temperature ($\gamma = 1$ and $\gamma = 9$, see Table 1). No WBF effect is considered here. In the liquid-only regime of the lower troposphere and down to about -20°C in the mixed-phase regime, no choice of parameters causes much dispersion and the value of the slope remains close to 8, the slope of the meteoric water line originally defined from precipitation samples by Craig (1961b). At higher altitudes and lower temperature, the deviation from the meteoric water line is significant and the choice of cloud parameters becomes important. In conditions close to ice saturation, the slope lies below 8, but at high supersaturations it can actually exceed 8.

Figure 10a shows how the differences in slope discussed above translate to differences between trajectories in $\delta\text{D}-\delta^{18}\text{O}$ space. It appears that the relative dispersion due to vapour saturation dominates that due to glaciation temperature. Greater separation with saturation is promoted at low temperature while the separation due to glaciation temperature is bounded by the converging slopes in Fig. 9. This dominance of sensitivity to supersaturation suggests that it may be possible to estimate its value from the joint measurement of δD and $\delta^{18}\text{O}$, regardless of the knowledge of the glaciation temperature. Such possibility is hampered by the sensitivity of the slope to the WBF process, as seen in Fig. 10b (where WBF is measured from the WBF fraction b of liquid to ice conversion). This sensitivity is concentrated in the temperature range $\sim -30^\circ\text{C}$

Vapour isotopic composition in updrafts

M. Bolot et al.

[Title Page](#)[Abstract](#)[Introduction](#)[Conclusions](#)[References](#)[Tables](#)[Figures](#)[◀](#)[▶](#)[◀](#)[▶](#)[Back](#)[Close](#)[Full Screen / Esc](#)[Printer-friendly Version](#)[Interactive Discussion](#)

Vapour isotopic composition in updrafts

M. Bolot et al.

Title Page

Abstract

Introduction

Conclusions

References

Tables

Figures

◀

▶

◀

▶

Back

Close

Full Screen / Esc

Printer-friendly Version

Interactive Discussion

to -40°C where WBF enhancement takes place and results in successive sign reversals of the generalised fractionation coefficients (as seen in Figs. 5c and 6c). Additional information can, however, be provided by parcel temperature: isotherms in the $\delta\text{D}-\delta^{18}\text{O}$ space depend on glaciation temperature and WBF fraction. The isotherms (see Figs. 10a and b) separate more with γ and b at warm temperatures where the iso- ζ curves merge than at low temperature where the iso- ζ curves separate. Consequently, one expects that the simultaneous measurement of δD , $\delta^{18}\text{O}$ and T provides a joint estimation of b and γ at warm temperature, leaving ζ fairly undetermined, whereas it provides an estimate of ζ but leaves b and γ fairly undetermined at low temperature. Any additional independent measurement or hypothesis that links the parameters would reduce the uncertainty. These properties are exploited in the next section.

The variability in the δD versus $\delta^{18}\text{O}$ relationship found in cold, glaciated regions of a rising convective system suggests that the commonly used metric of deuterium excess (d), originally defined by (Dansgaard, 1964) as $d = \delta\text{D} - 8\delta^{18}\text{O}$ to account for kinetic effects in meteoric water formation and precipitation, may be highly sensitive to in-cloud processes. Any deviation from the value 8 in Fig. 9 is indicative of a positive or negative tendency in deuterium excess.

Profiles of d along parcel trajectories exhibit both vertical structure and sensitivity to assumptions about cloud processes. Figure 11 shows the sensitivity of d to saturation, glaciation parameter, and the WBF effect. From the boundary layer to about -20°C , d is roughly constant at $d \approx 10\text{‰}$ in all simulations, because the slope $d\delta\text{D}/d\delta^{18}\text{O}$ stays close to 8 (as shown in Fig. 9). In the mid- to upper troposphere (11–15 km), however, modelled d -excess shows wide variations, ranging from -200 to $+300\text{‰}$. d in this region is reduced by larger supersaturations, higher glaciation altitudes, and increased WBF, with some combinations driving d negative, typically at convective detrainment levels. In the tropopause transition region (above 15 km), modelled d is positive in nearly all conditions but with variations of up to a thousand permil depending on cloud processes.

Vapour isotopic composition in updrafts

M. Bolot et al.

Title Page

Abstract

Introduction

Conclusions

References

Tables

Figures

◀

▶

◀

▶

Back

Close

Full Screen / Esc

Printer-friendly Version

Interactive Discussion



The vertical structure and sensitivity in d may make it a useful tracer of cloud processes, but care must be taken to understand the factors that affect it. Several recent modelling studies (Bony et al., 2008; Blossey et al., 2010; Kurita et al., 2011) have used d as a tracer of upper tropospheric air subsiding to the surface, while using simplified parameterized physics of vapour saturation. In global models $S_i = 1 - \lambda T [^\circ\text{C}]$ is often used (Hoffmann et al., 1998; Schmidt et al., 2007; Lee et al., 2007; Yoshimura et al., 2008; Tindall et al., 2009; Risi et al., 2010; Kurita et al., 2011) as discussed in Sect. 4.1. Spanning the range of λ used across these studies, assuming a glaciation temperature of $\sim -15^\circ\text{C}$ and no WBF, yields d-excess in convective cores that increase monotonically with altitude to reach values of 20–130‰ between 12 and 14 km (see Fig. 11). These values are grossly consistent with our scenarii where $\zeta \sim 0.4 - 0.5$, that saturate at 18–23% over ice below -40°C . However, as discussed throughout this paper, physical processes may well vary outside those assumptions, which would yield very different values of d-excess at low temperature.

Our prediction is that low or negative values of d-excess could be found in and near convective clouds at detrainment levels given conditions of high supersaturation, high glaciation altitude, and a significant WBF effect. In particular, vapour-limited conditions that could take place in stratiform anvils and promote supercooled droplet evaporation should be marked by a shift of up to -100% in the deuterium-excess of vapour. We stress that a better understanding of the drivers of d-excess variations is important for the interpretation of field measurements.

6 Towards a retrieval of physical parameters from water isotopologues

The modelling framework presented here allows us to test quantitatively how combined observations of water vapour $\delta^{18}\text{O}$ and δD at several altitudes can provide informations about in-cloud conditions, including vapour supersaturation and the profile of (isotopically active) cloud liquid water. Although the environment of a convective core means that it is unlikely that in-situ measurements can be obtained there, it is possible that

observational data will be achievable at cloud base (or in the boundary layer air being entrained) and at cloud top (in the range 12 to 14 km typically). We therefore look for cases in which isotopic observations at these altitudes can provide information about cloud processes. We do not seek to be exhaustive as our main purpose is illustrative.

To evaluate whether this type of measurement campaign can provide insight into convective physics, we test the utility of these isotopic measurements in retrieving three arbitrarily chosen parameters of interest: ζ , which measures vapour saturation; $r_1[-20^\circ\text{C}]$, the abundance of supercooled water at -20°C and T_g , the temperature of full glaciation defined as $T_g = T [r_1 = 10^{-6}]$ (supercooled water content and glaciation temperature depend on the parameters C_1 and γ in our model; see Table 1). We combine the cloud base and cloud top measurements into two composite “observables” chosen to be particularly sensitive to cloud saturation and to cloud liquid water profile, respectively. The saturation-sensitive observable quantity is defined as $\Psi = \ln \left(\frac{R_v^{18\text{O}}(\text{top})}{R_v^{18\text{O}}(\text{gnd})} \right) / \ln \left(\frac{R_v^{\text{D}}(\text{top})}{R_v^{\text{D}}(\text{gnd})} \right)$ where “top” and “gnd”, respectively denote cloud top and cloud base observations; the liquid-sensitive observable quantity is defined as $\Pi = \ln \left(\frac{R_v^{\text{D}}(\text{top})}{R_v^{\text{D}}(\text{gnd})} \right)$, which contains information on the vertical profile of cloud liquid water.

Owing to the complexity of in-cloud isotopic physics, even within our model, there is no simple deterministic relation between these isotopic observables and cloud parameters: the problem is underdetermined. We can however examine the statistical relationship between composite observables and parameters to be retrieved, taking into account the ranges of possible values for all unknown cloud parameters. We set up a Monte Carlo simulation, varying our control parameters ζ , C_1 , γ , and b , as well as the values of vapour isotopic composition at cloud base δ_0^{D} and $\delta_0^{18\text{O}}$. These parameters are treated as independent random variables and sampled from uniform distributions

Vapour isotopic composition in updrafts

M. Bolot et al.

Title Page

Abstract

Introduction

Conclusions

References

Tables

Figures

◀

▶

◀

▶

Back

Close

Full Screen / Esc

Printer-friendly Version

Interactive Discussion



(\mathcal{U}) over plausible ranges of values:

$$P(\zeta) = \mathcal{U}([0, 1]),$$

$$P(C_l) = \mathcal{U}([0, 0.5]),$$

$$P(\gamma) = \mathcal{U}([1, 9]),$$

$$P(b) = \mathcal{U}([0, 1]),$$

$$P(\delta_0\text{D}) = \mathcal{U}([-90\text{‰}, -70\text{‰}]),$$

$$P(\delta_0^{18}\text{O}) = \mathcal{U}([-15\text{‰}, -10\text{‰}]).$$

Uniform distribution is the simplest possible choice for this study. If more realistic distributions were available, the process followed here would easily be adapted to incorporate that increase in knowledge. We generate 10^6 simulations and then use a kernel-based method (Botev et al., 2010) to estimate the joint probability densities of composite observables Ψ and Π with relevant cloud parameters: $\rho(\zeta, \Psi)$, $\rho(T_g, \Pi)$ and $\rho(r_l[-20^\circ\text{C}], \Pi)$.

Figure 12 shows the joint distributions estimated from that procedure at 12 and 14 km. In many cases, a compact relation emerges, indicating that isotopic measurements provide robust tracers of cloud parameters. Relationships are generally stronger at one altitude than another. Supersaturation is more readily retrieved at higher altitudes, where the footprint of signals from the various processes involved in cloud glaciation has partially vanished, and parameters associated with cloud glaciation are, logically enough, more readily retrieved at lower altitudes, closer to the glaciation region. The saturation parameter ζ is essentially linear with Ψ at both altitudes (panels a and d), but the relationship is tighter at 14 km than at 12 km. Isotopic measurements at 12 km, conversely, are better tracers of glaciation temperature T_g (b and e) and liquid water content $r_l[-20^\circ\text{C}]$ (c and f) than measurements performed at 14 km. These results are consistent with inferences about the use of $\delta^{18}\text{O}$ and δD measurements drawn in Sect. 5.

Vapour isotopic composition in updrafts

M. Bolot et al.

Title Page

Abstract

Introduction

Conclusions

References

Tables

Figures

◀

▶

◀

▶

Back

Close

Full Screen / Esc

Printer-friendly Version

Interactive Discussion



Vapour isotopic composition in updrafts

M. Bolot et al.

Title Page

Abstract

Introduction

Conclusions

References

Tables

Figures

◀

▶

◀

▶

Back

Close

Full Screen / Esc

Printer-friendly Version

Interactive Discussion



A finer analysis shows that processes controlling liquid to ice transition (i.e. γ , b) and auto-conversion (i.e. C_1) compete to broaden the joint distributions $\rho(T_g, \Pi)$ and $\rho(r_1[-20^\circ\text{C}], \Pi)$. In practice, these joint statistics can be improved by incorporating a priori information on cloud processes (e.g. precipitation radar, CAPE estimation), which is essentially equivalent to reducing the Monte Carlo sampling to a subset of cases. A full treatment of observations should also involve a Bayesian analysis that takes into account observational errors. Such developments are beyond the scope of this paper. Our purpose here is to give evidence as to how a carefully designed observational campaign that measures isotopic composition of water vapour in air that has been processed by clouds can provide insights into previously hidden convective processes.

7 Conclusions

This work revisits the basic processes setting the isotopic composition of water vapour in a rising unmixed air parcel, with a consistent and physically-based treatment of microphysics and thermodynamics over vapour, liquid water and cloud ice. It is motivated by the current trend in the literature to investigate cloud processes from isotopic measurements (Fudeyasu et al., 2008; Lawrence and Gedzelman, 1996, 2003; Risi et al., 2008; Kurita et al., 2011; Berkelhammer et al., 2012) and the need to reexamine some widely used assumptions regarding convective physics in global models. By investigating the sensitivity of isotopic composition to relevant parameters of cloud physics, this work also suggests new ways to estimate these parameters from carefully designed measurements of isotopologues. We limit the scope of this study to updraft physics and its intrinsic variability, and for this reason consider the boundary layer conditions as fixed and neglect any process related to evaporation of precipitations and entrainment.

We show that isotopic kinetic effects at evaporation/deposition are driven not only by the differential molecular diffusivity between light and heavy isotopologues, as is

sometimes suggested, but also by the preferential uptake of heavy isotopologues at condensate surface. Both effects conspire to set up gradients in molecular abundance across a diffusive boundary layer surrounding condensate, that differ between heavy and light isotopologues. We also show that the magnitude of isotopic kinetic effects is reduced by thermal impedance to crystal growth/droplet evaporation, in a way that vanishes with altitude.

Model simulations replicate the well-known regime transition between warm, liquid-only clouds where vapour isotopic changes are buffered to some extent by re-equilibration with liquid water, and cold, fully glaciated clouds in which isotopic evolution is essentially pure Rayleigh distillation, modified only by the kinetic effects associated with the growth of ice particles. The dominant convective variables affecting vapour isotopic composition are the profile of supercooled water in active equilibrium with vapour within the intervening mixed-phase regime (between 0 °C and -40 °C), the supersaturation over ice in the ascending air parcel (and attendant subsaturation over liquid water), which governs kinetic modifications to isotopic fractionation, and the route to cloud glaciation (through the Wegener-Bergeron-Findeisen WBF process versus heterogeneous freezing). These parameters are affected by the number density of cloud particles and the updraft speed of the rising air parcel. In particular, the size of the supercooled liquid water reservoir in isotopic balance with vapour depends on droplets spectra and updraft strength. In the mixed-phase region, we show that glaciation by the WBF process, which is expected to occur in vapour limited conditions, may produce an isotopic enhancement provided supercooled droplets have survived to very low temperatures (-30 °C to -40 °C). This effect is strong for the system H₂¹⁸O/H₂O and, consequently, may produce a shift in d-excess of up to -100‰. Such conditions may happen during transition from active convection to decaying stratiform stage.

Since severe turbulence, hail and icing conditions are ubiquitous within active convective cores, in-situ sampling of such environments comes at a very high risk. The fact that water vapour within convective systems and their immediate surrounding has acquired its isotopic composition in updrafts opens a way to probe their physics in

Vapour isotopic composition in updrafts

M. Bolot et al.

[Title Page](#)[Abstract](#)[Introduction](#)[Conclusions](#)[References](#)[Tables](#)[Figures](#)[⏪](#)[⏩](#)[◀](#)[▶](#)[Back](#)[Close](#)[Full Screen / Esc](#)[Printer-friendly Version](#)[Interactive Discussion](#)

Vapour isotopic composition in updrafts

M. Bolot et al.

Title Page

Abstract

Introduction

Conclusions

References

Tables

Figures

◀

▶

◀

▶

Back

Close

Full Screen / Esc

Printer-friendly Version

Interactive Discussion



a remote way. We have described how measurements of δD and $\delta^{18}O$ at cloud base and over restricted altitude regions at cloud top can be combined to perform estimations of supersaturation and supercooled liquid water contents within updrafts. The fact that in-cloud measurements are not required means that measurement requirements are greatly simplified, and can facilitate planning future measurement strategies. Cloud base measurements can be easily obtained from ground-based instruments and cloud top measurements would be possible from aircraft campaigns (Hanisco et al., 2007; Sayres et al., 2010) or even remotely, by absorption in the mid-infrared (Nassar et al., 2007; Randel et al., 2012), active microwave limb sounding (Kursinski et al., 2004), or possibly by far-infrared thermal emission (Herbin et al., 2009). If measuring the isotopic composition of vapour at cloud top is sufficient, then a relatively tractable measurement program using existing techniques may permit diagnosing aspects of cloud dynamics from space.

Appendix A

Diffusional growth rate of droplets and ice crystals

We consider a single droplet or an ice crystal of mass m , growing by diffusion of water vapour to its surface. We further assume that the droplet or crystal is already grown from its nucleus and that its temperature is homogeneous. We assume the contribution of heavy isotopologues is small, so that m corresponds to the mass of light water within the condensate. The rate of mass accretion according to stationary diffusion theory is then given by Pruppacher and Klett (1978) as:

$$\frac{dm}{dt} = K_v f_v \int_S \vec{\nabla} \rho_v \cdot \vec{d}^2 \sigma = -4\pi C K_v f_v \left(\rho_v^{(s)} - \rho_v^{(\infty)} \right), \quad (\text{A1})$$

where (s) stands for the surface of the droplet or the ice crystal and (∞) for the far field environment, C is the droplet radius or crystal capacitance (an effective radius for

diffusional growth that depends only on the geometry of the crystal), K_v is the molecular diffusivity of light vapour and f_v is the ventilation coefficient for light vapour that describes enhancement of mass accretion over pure diffusive theory owing to the condensate fall relatively to the air. The light vapour density field ρ_v satisfies the stationary

5 Laplace equation $\nabla^2 \rho_v = 0$ with boundary conditions $\rho_v = \rho_v^{(s)}$ at the surface of the condensate and $\rho_v = \rho_v^{(\infty)}$ in the far field. Equation (A1) holds for both deposition, when $\rho_v^{(s)} < \rho_v^{(\infty)}$, and evaporation, when $\rho_v^{(s)} > \rho_v^{(\infty)}$.

We assume here a scale separation between sub-millimetric diffusive processes and hydrodynamics, so that the far field values of vapour concentration $\rho_v^{(\infty)}$ and temperature $T^{(\infty)}$ are equivalent to the macroscopic values in the air parcel being modelled. This approximation might be questionable in highly turbulent regions of convective clouds (Lanotte et al., 2009).

We assume also that phase equilibrium applies at the surface of the droplet or the ice crystal. In this case surface vapour concentration corresponds to saturation at surface temperature and pressure: $\rho_v^{(s)} = \rho_{\text{sat}}^{l,i}[T^{(s)}, \rho]$, where $T^{(s)}$ is the surface temperature of the condensate and “sat” stands for the equilibrium saturation value at the indicated temperature and pressure. This assumption on $\rho_v^{(s)}$ breaks down for very small droplets (essentially unactivated aerosols) when surface curvature and salt concentration effects cannot be ignored, but those conditions can be neglected in isotopic models since total water content in particles this small is negligible compared to remaining vapour and so has negligible isotopic effect. Further comments on the growth of ice crystals are provided at the end of this section.

The accretion or evaporation represented by Eq. (A1) is associated with a corresponding release or intake of latent heat $dQ/dt = -L_{l,i} dm/dt$ (where $L_{l,i}$ is the latent heat of vaporisation or sublimation). Continuity of the heat flow at the surface of the particle requires that this heat source is balanced by the diffusive flux of heat between the particle and its environment. This balance holds because the rate of heat storage accommodating the variation of particle temperature as it rises within the cloud is

Vapour isotopic composition in updrafts

M. Bolot et al.

[Title Page](#)[Abstract](#)[Introduction](#)[Conclusions](#)[References](#)[Tables](#)[Figures](#)[◀](#)[▶](#)[◀](#)[▶](#)[Back](#)[Close](#)[Full Screen / Esc](#)[Printer-friendly Version](#)[Interactive Discussion](#)

negligible compared to the rate of latent heat release and that of diffusive heat export, as evidenced by the smallness of thermal relaxation times (Mason, 1956, see also Appendix D and Fig. B1). Heat diffusion can then be handled in the same way as vapour diffusion since the underlying physical processes are formally equivalent. Hence, we have:

$$\frac{dQ}{dt} = -L_{l,i} \frac{dm}{dt} = k_h f_h \int_S \vec{\nabla} T \cdot d^2\sigma = -4\pi C k_h f_h (T^{(s)} - T^{(\infty)}). \quad (\text{A2})$$

The temperature field satisfies $\nabla^2 T = 0$ with boundary conditions $T = T^{(s)}$ at the surface of the condensate and $T = T^{(\infty)}$ in the far field. k_h is the thermal conductivity of moist air and f_h is the thermal ventilation coefficient.

Replacing Eq. (A1) in Eq. (A2) yields:

$$k_h f_h (T^{(s)} - T^{(\infty)}) = -L_{l,i} K_v f_v (\rho_v^{(s)} - \rho_v^{(\infty)}), \quad (\text{A3})$$

which shows that the surface temperature of the condensate is raised above the environmental temperature during deposition, or lowered below it during evaporation, as expected.

Since water vapour at the particle surface is assumed to be at saturation, $\rho_v^{(s)} - \rho_v^{(\infty)}$ can be expressed as a function of densities at saturation and then expanded to first order in $T^{(s)} - T^{(\infty)}$ by using the Clausius-Clapeyron relation, leading to

$$\rho_v^{(s)} - \rho_v^{(\infty)} \sim \rho_{\text{sat}}^{l,i(\infty)} \left(1 + \frac{1}{T^{(\infty)}} \left(\frac{L_{l,i}}{R_v^* T^{(\infty)}} - 1 \right) (T^{(s)} - T^{(\infty)}) - S_{l,i} \right), \quad (\text{A4})$$

where $\rho_{\text{sat}}^{l,i(\infty)}$ is shorthand for $\rho_{\text{sat}}^{l,i} [T^{(\infty)}, p]$ and $S_{l,i} = \rho_v^{(\infty)} / \rho_{\text{sat}}^{l,i(\infty)}$ is the relative humidity of the air parcel over liquid water or ice.

The rate of mass accretion for droplets or ice crystals can be then rewritten as a function of parcel temperature only by solving for $\rho_v^{(s)} - \rho_v^{(\infty)}$ from Eq. (A3) and Eq. (A4),

Vapour isotopic composition in updrafts

M. Bolot et al.

Title Page

Abstract

Introduction

Conclusions

References

Tables

Figures

◀

▶

◀

▶

Back

Close

Full Screen / Esc

Printer-friendly Version

Interactive Discussion



and then replacing it in Eq. (A1) (Mason, 1971):

$$\frac{dm}{dt} = -4\pi C f_v K_v (1 - S_{l,i}) A_{l,i} \rho_{\text{sat}}^{l,i(\infty)}, \quad (\text{A5})$$

$$\text{with } A_{l,i} = \left[1 + \frac{f_v K_v L_{l,i} \rho_{\text{sat}}^{l,i(\infty)}}{f_h k_h T^{(\infty)}} \left(\frac{L_{l,i}}{R_v^* T^{(\infty)}} - 1 \right) \right]^{-1}. \quad (\text{A6})$$

- 5 The $A_{l,i}$ are transfer coefficients between vapour and condensate that represent reduced mass accretion (or loss) owing to the need to extract (or provide) latent heat of condensation (or evaporation) across the diffusive boundary layer.

The impeding effect of thermal diffusion on crystal growth varies with altitude in the cloud. From Eqs. (A3) and (A4), the temperature difference across the boundary layer
10 may be obtained and arranged as follows:

$$T^{(s)} - T^{(\infty)} = - \underbrace{\frac{L_{l,i}}{c_p}}_1 (1 - S_{l,i}) \underbrace{\frac{f_v}{Le f_h}}_2 q_{\text{sat}}^{l,i(\infty)} \underbrace{\left[1 + \frac{L_{l,i}}{c_p} \frac{f_v}{Le f_h} \frac{1}{T^{(\infty)}} \left(\frac{L_{l,i}}{R_v^* T^{(\infty)}} - 1 \right) q_{\text{sat}}^{l,i(\infty)} \right]^{-1}}_{A_{l,i}}, \quad (\text{A7})$$

where $q_{\text{sat}}^{l,i(\infty)} = \rho_{\text{sat}}^{l,i(\infty)} / \rho^{(\infty)}$ is the saturation specific humidity with respect to liquid water or ice, measured in the far field, and the Lewis number $Le = K_h / K_v$ measures the ratio between thermal and molecular diffusivity. (Thermal diffusivity K_h is defined by
15 $k_h = \rho^{(\infty)} c_p K_h$). It can be shown from the kinetic theory of gases that Le is a function of gas mixture composition only (i.e. it is independent of temperature and pressure), and that term 2 of Eq. (A7) is close to 1 (see Supplement). Term 1 is weakly dependent on temperature and the strong decrease of $q_{\text{sat}}^{l,i(\infty)}$ with decreasing temperature

Vapour isotopic composition in updrafts

M. Bolot et al.

Title Page

Abstract

Introduction

Conclusions

References

Tables

Figures

◀

▶

◀

▶

Back

Close

Full Screen / Esc

Printer-friendly Version

Interactive Discussion



Vapour isotopic composition in updrafts

M. Bolot et al.

Title Page

Abstract

Introduction

Conclusions

References

Tables

Figures

◀

▶

◀

▶

Back

Close

Full Screen / Esc

Printer-friendly Version

Interactive Discussion



(see Appendix C1) dominates the temperature dependency of term 3. Thus, thermal impedance to crystal growth depends on altitude mostly through $S_{l,i}$ (it vanishes at exact saturation) and $q_{\text{sat}}^{l,i(\infty)}$. For the sake of illustration, consider a cloud parcel at -20°C (8.5 km a.g.l.) with 10 % supersaturation over ice. In these conditions, our model (see Sect. 3.2.4) shows that growing crystals are heated 0.4°C above $T^{(\infty)}$, evaporating droplets are cooled 0.4°C below $T^{(\infty)}$ and $A_{l,i}$ is ~ 0.65 , so the crystal growth is reduced. As the parcel rises within the cloud and its temperature drops, the temperatures at droplet surface approach that of the environment ($T^{(s)} - T^{(\infty)}$ eventually vanishes) and $A_{l,i}$ approaches unity, i.e. crystal growth is no longer impeded by heat diffusion.

Appendix B

Derivation of the kinetic fractionation factor and isotopic relaxation time for droplets and ice

The kinetic modification to the fractionation factor can be derived from considering the accretion of heavy and light isotopologues separately. Since diffusion of all water isotopologues is governed by the same physics, the rate of accretion of a heavy water isotopologue onto a cloud droplet or crystal can be written analogously to that for light isotopes (cf. Eq. A1):

$$\frac{dm'}{dt} = -4\pi CK'_v f'_v \left(\rho'_{v^{(s)}} - \rho'_{v^{(\infty)}} \right), \quad (\text{B1})$$

where m' is the mass of the heavy isotopologue within the droplet, $\rho'_{v^{(s)}}$ and $\rho'_{v^{(\infty)}}$ are the densities of the heavy isotopologue vapour at the surface of the droplet and in the air parcel, K'_v is molecular diffusivity of the heavy vapour, and f'_v is the corresponding coefficient.

In the case of a droplet, equilibrium fractionation is assumed to apply at its surface, thus $R_v^{(s)} = R_l^{(s)} / \alpha_l$, where $R_l^{(s)}$ is the isotopic ratio of liquid water at the droplet surface. (As stated in Appendix A, this assumption is reasonable for droplets much larger than the size of the initial condensation nucleus). We can then express the vapour pressure of heavy water isotopologues as $\rho_v'^{(s)} = R_l^{(s)} \rho_v^{(s)} / \alpha_l$. If we then take $\rho_v^{(s)}$ from Eq. (A4), Eq. (B1) becomes:

$$\frac{dm'}{dt} = -4\pi C K_v' f_v' \left[S_l \left(\frac{R_l^{(s)}}{\alpha_l} - R_v^{(\infty)} \right) + A_l (1 - S_l) \frac{R_l^{(s)}}{\alpha_l} \right] \rho_{\text{sat}}^{l(\infty)}. \quad (\text{B2})$$

The evolution of the isotopic ratio R_l for the whole droplet can now be derived from Eqs. (A5) and (B2) by assuming an homogeneous isotopic composition within the droplet, a reasonable assumption given the fast self-diffusion of liquid water (Wang, 1951b). With this assumption, the surface isotopic composition holds for the whole droplet, that is $R_l^{(s)} = R_l$ and $R_l = m' / m$. It is also reasonable to further assume a spherical droplet of some radius a , in which case the effective radius C becomes a and the mass $m = \frac{4}{3}\pi a^3 \rho_{\text{drop}}$. Then the tendency on droplet isotopic ratio becomes:

$$\begin{aligned} \frac{dR_l}{dt} &= \frac{1}{m} \left(\frac{dm'}{dt} - R_l \frac{dm}{dt} \right) \\ &= -\frac{3\rho_{\text{sat}}^{l(\infty)}}{a^2 \rho_{\text{drop}}} \left[K_v' f_v' \left(S_l \left(\frac{R_l}{\alpha_l} - R_v^{(\infty)} \right) + A_l (1 - S_l) \frac{R_l}{\alpha_l} \right) - K_v f_v R_l A_l (1 - S_l) \right]. \end{aligned} \quad (\text{B3})$$

Equation (B3) is equivalent to Eq. (5) of Jouzel et al. (1975), and to Eq. (20) of Gedzelman and Arnold (1994) if their $(1 + b)$ is replaced by A_l^{-1} . Equation (B3) can be seen as an adjustment of droplet isotopic composition, if rewritten as:

$$\frac{dR_l}{dt} = -\frac{R_l}{\tau_{\text{drop}}} + \frac{3\rho_{\text{sat}}^{l(\infty)}}{a^2 \rho_{\text{drop}}} K_v' f_v' S_l R_v^{(\infty)}, \quad (\text{B4})$$

Vapour isotopic composition in updrafts

M. Bolot et al.

Title Page

Abstract

Introduction

Conclusions

References

Tables

Figures

◀

▶

◀

▶

Back

Close

Full Screen / Esc

Printer-friendly Version

Interactive Discussion



The factor τ_{drop} is then an e-folding time of droplet isotopic relaxation to equilibrium with its environment:

$$\tau_{\text{drop}} = \underbrace{\frac{a^2 \rho_{\text{drop}} \alpha_l}{3 \rho_{\text{sat}}^{l(\infty)} K'_V f'_V}}_1 \left[\underbrace{(S_l + A_l (1 - S_l)) - \alpha_l \frac{K_V f_V}{K'_V f'_V} A_l (1 - S_l)}_2 \right]^{-1}. \quad (\text{B5})$$

The degree of adjustment depends on droplet size, vapour saturation and altitude within the cloud. In a liquid-saturated environment (i.e. $S_l = 1$), τ_{drop} reduces to the underbraced term 1 of Eq. (B5), which is also the relaxation time for stationary droplets as defined by Jouzel et al. (1975) and Stewart (1975). In this case, the kinetic theory of gases under the rigid elastic spheres approximation (Chapman and Cowling, 1970) predicts that τ_{drop} behaves as $a^2 / \left(q_{\text{sat}}^{l(\infty)} T^{1/2} \right)$ (neglecting variations of the fractionation coefficient with temperature). Decreasing temperature and saturation specific humidity at greater altitudes within the cloud slow down isotopic exchanges between droplets and vapour, as illustrated on Fig. B1.² It must be added that supercooled droplets are likely to evaporate in a liquid-sub-saturated environment (i.e. $S_l < 1$), so that in sub-saturated environments, diffusion of vapour out of the droplets (term 2 of Eq. B5) further lengthens isotopic relaxation times.

To provide some perspective on the question of droplet adjustment, note that the isotopic equilibration of droplets with the surrounding vapour depends on temperature and size, but also on the updraft speed. For instance, a supercooled droplet of radius 30 μm has an isotopic relaxation time between 14 s and 20 s at -30°C , depending on whether vapour is at saturation over liquid water or ice. If carried upward in a fast updraft, the droplet can accumulate a significant isotopic imbalance with surrounding vapour. To understand how the validity of isotopic relaxation assumptions depends on

²Note that Jouzel et al. (1975) compute τ_{drop} at surface pressure, which yields values over-estimated by up to 300 %.

Vapour isotopic composition in updrafts

M. Bolot et al.

Title Page

Abstract

Introduction

Conclusions

References

Tables

Figures

◀

▶

◀

▶

Back

Close

Full Screen / Esc

Printer-friendly Version

Interactive Discussion



Vapour isotopic composition in updrafts

M. Bolot et al.

Title Page

Abstract

Introduction

Conclusions

References

Tables

Figures

◀

▶

◀

▶

Back

Close

Full Screen / Esc

Printer-friendly Version

Interactive Discussion



updraft vertical speed w_{up} , consider that $w_{\text{up}}\tau_{\text{drop}}$ is the relevant vertical scale of isotopic adjustment. For instance, in order to relax over a maximum vertical scale of 10 m in a stream of 10 ms^{-1} , a droplet must satisfy $\tau_{\text{drop}} = 1\text{ s}$ at most. As cloud temperature drops, this requirement is only satisfied by droplets of increasingly smaller radius: droplets should be no larger in radius than $20\text{ }\mu\text{m}$ at $-4\text{ }^\circ\text{C}$, $10\text{ }\mu\text{m}$ at $-22\text{ }^\circ\text{C}$ and $5\text{ }\mu\text{m}$ at $-36\text{ }^\circ\text{C}$ (as illustrated in Fig. B1). Faster updraft speeds would yield even smaller critical radii. It is thus expected that only a fraction of cloud liquid water fully re-equilibrates with surrounding vapour and that this portion decreases at lower temperatures. (see also discussion in Sect. 4.1).

The cloud water droplets that adjust rapidly to their environment through their diffusive layer reach a stationary isotopic pseudo-equilibrium:

$$R_1^{(\text{eq})} = \frac{\alpha_l S_l R_v^{(\infty)}}{(S_l + A_l(1 - S_l)) - \alpha_l \frac{K_v f_v}{K_v' f_v'} A_l(1 - S_l)}. \quad (\text{B6})$$

Following Ciais and Jouzel (1994), this pseudo-equilibrium condition can be written as an effective kinetic fractionation factor between cloud water and vapour, defining $\alpha_{\text{kl}}^{(\text{eq})} = R_1^{(\text{eq})}/R_v^{(\infty)}$. By introducing the effective saturation over liquid water $S_l^{(\text{eff})} = [1 - A_l(1 - S_l^{-1})]^{-1}$, as in Jouzel and Merlivat (1984)³, Eq. (B6) can be rearranged to give:

$$\alpha_{\text{kl}}^{(\text{eq})} = \frac{\alpha_l}{1 + (\beta_l - 1)(1 - (S_l^{(\text{eff})})^{-1})}, \quad (\text{B7})$$

with $\beta_l = \alpha_l \frac{K_v f_v}{K_v' f_v'}$.

³It appears that the definition of A_l in this work is reversed from its initial expression in Jouzel et al. (1975).

The kinetic theory for ice is similar to that for cloud water, with one critical difference, that ice does not homogenize isotopically. The rate of accretion of heavy isotopologues is again given by:

$$\frac{dm'}{dt} = -4\pi CD'_V f'_V \left[S_i \left(\frac{R_i^{(s)}}{\alpha_i} - R_V^{(\infty)} \right) + A_i (1 - S_i) \frac{R_i^{(s)}}{\alpha_i} \right] \rho_{\text{sat}}^{i(\infty)}, \quad (\text{B8})$$

5 which is identical to Eq. (B2) other than the use of indices i to denote ice rather than l . However, because the diffusivity within ice crystal lattice is slow – Kuhn and Thürkauf (1958) have measured a diffusivity of HDO in ice of only $10^{-14} \text{ m}^2 \text{ s}^{-1}$ – isotopic equilibrium between vapour and a whole ice crystal will not occur over any reasonable timescale during the life-cycle of a cloud. The mean isotopic ratio within an ice crystal, $R_i^{(c)} = m'/m$, then depends on the growth history of the crystal. Unlike in the liquid case, isotopic pseudo-equilibrium holds only between vapour and the most external layer of the crystal, and there is no transient to that state.

The condition of equilibrium at the ice surface yields:

$$R_i^{(s)} = \frac{dm'/dt}{dm/dt}. \quad (\text{B9})$$

15 The instantaneous kinetic fractionation factor between ice surface and vapour within the air parcel $\alpha_{ki} = R_i^{(s)}/R_V^{(\infty)}$ can then be readily derived upon replacing Eq. (B9) in Eq. (B8), using Eq. (A5) and re-arranging:

$$\alpha_{ki} = \frac{\alpha_i}{1 + (\beta_i - 1) \left(1 - (S_i^{(\text{eff})})^{-1} \right)}, \quad (\text{B10})$$

20 where $S_i^{(\text{eff})} = \left[1 - A_i \left(1 - S_i^{-1} \right) \right]^{-1}$ is the effective saturation over ice taken at the temperature of the air parcel and $\beta_i = \alpha_i \frac{K_V f_r}{K'_V f'_r}$. Equation (B10) corresponds to Eq. (14) of
22500

Vapour isotopic composition in updrafts

M. Bolot et al.

Title Page

Abstract

Introduction

Conclusions

References

Tables

Figures

◀

▶

◀

▶

Back

Close

Full Screen / Esc

Printer-friendly Version

Interactive Discussion



Jouzel and Merlivat (1984). Note that the expression of α_{ki} is formally equivalent to that of $\alpha_{kl}^{(eq)}$ although there is no global equilibrium in this case.

Since f_v/f'_v and f_v/f_h do not deviate from 1 by more, respectively, than 0.5 % and 2 % over all circumstances (see Supplement Sect. 1), we systematically set these ratios to 1 in our computations of kinetic fractionation factors.

Appendix C

Thermodynamic and isotopic quantities

C1 Thermodynamic expressions

We summarize here the standard thermodynamic expressions and constants used in this study.

Values of thermodynamic specific capacities and gas constants:

$$R_v^* = 461 \text{ J kg}^{-1} \text{ K}^{-1},$$

$$R_d^* = 287 \text{ J kg}^{-1} \text{ K}^{-1},$$

$$c_{pv} = 1885 \text{ J kg}^{-1} \text{ K}^{-1},$$

$$c_l = 4186 \text{ J kg}^{-1} \text{ K}^{-1},$$

$$c_i = 2106 \text{ J kg}^{-1} \text{ K}^{-1},$$

$$\text{with } \epsilon = R_d^*/R_v^* = 0.622.$$

Latent heats:

$$L_{l(0)} = 2.501 \times 10^6 \text{ J kg}^{-1}, \quad L_l = L_{l(0)} - (c_l - c_{pv})(T - 273.15),$$

$$L_{i(0)} = 2.836 \times 10^6 \text{ J kg}^{-1}, \quad L_i = L_{i(0)} - (c_i - c_{pv})(T - 273.15).$$

Vapour isotopic composition in updrafts

M. Bolot et al.

Title Page

Abstract

Introduction

Conclusions

References

Tables

Figures

◀

▶

◀

▶

Back

Close

Full Screen / Esc

Printer-friendly Version

Interactive Discussion



Saturation vapour pressure over liquid, after Murphy and Koop (2005) (unit Pa):

$$e_{(\text{sat})}^l = \exp\left(54.842763 - \frac{6763.22}{T} - 4.210\ln(T) + 0.000367T + \tanh(0.0415(T - 218.8))\left(53.878 - \frac{1331.22}{T} - 944523\ln(T) + 0.014025T\right)\right). \quad (\text{C1})$$

- 5 This expression is given as accurate within 0.05% between 123K and 332K.
Saturation vapour pressure over ice, after Murphy and Koop (2005) (unit Pa):

$$e_{(\text{sat})}^i = \exp\left(9.550426 - \frac{5723.265}{T} + 3.53068\ln(T) - 0.00728332T\right). \quad (\text{C2})$$

- 10 Ice density is fixed at $\rho_{\text{ice}} = 0.9 \times 10^3 \text{ kg m}^{-3}$, which corresponds to pure water composition without any included air.

- Note that the expression of θ_{il} given in Eq. (5) is strictly valid only for fixed thermodynamic capacities while Eqs. (C1) and (C2) take into account the variation of the thermodynamic capacities with temperature. This small inconsistency has no practical effect for temperature computation, but allows more accurate expression of vapour sub-/supersaturation in kinetic fractionation factors.

C2 Reference isotopic ratio

- 20 The reference isotopic ratio of deuterium for VSMOW is provided in the literature (Hagemann et al., 1970) as a ratio of abundances of deuterium to hydrogen $[D]/[H]$ and takes the value $1.5576 \pm 0.0005 \times 10^{-4}$. In this study, we consider the ratio of mass of HDO to H_2O , which involves a multiplication by a factor two and by the ratio of molecular mass of HDO to H_2O , i.e. 19/18. Hence we have $R_0[\text{HDO}/\text{H}_2\text{O}] = 3.2891 \times 10^{-4}$. In the same way, the VSMOW reference isotopic ratio of oxygen-18 as found in the literature is transformed to $R_0[\text{H}_2^{18}\text{O}/\text{H}_2\text{O}] = 22.28 \times 10^{-4}$ in our study.

C3 Equilibrium fractionation

The equilibrium fractionation factors depend only on temperature and have been measured in laboratory for HDO/H₂O by Merlivat and Nief (1967) who provide the following semi-empirical expressions, based on measurements made between -11°C and 5.5°C for liquid-vapour phase transition and between -33°C and -6°C for ice-vapour phase transition:

$$\alpha_l(\text{HDO}/\text{H}_2\text{O}) = \exp\left(\frac{15013}{T^2} - 0.1\right), \quad (\text{C3})$$

$$\alpha_i(\text{HDO}/\text{H}_2\text{O}) = \exp\left(\frac{16289}{T^2} - 0.0945\right). \quad (\text{C4})$$

The corresponding expressions for H₂¹⁸O/H₂O have been obtained by Majoube (1971) and Majoube (1970), yielding:

$$\alpha_l(\text{H}_2^{18}\text{O}/\text{H}_2\text{O}) = \exp\left(\frac{1137}{T^2} - \frac{0.4156}{T} - 0.0020667\right), \quad (\text{C5})$$

$$\alpha_i(\text{H}_2^{18}\text{O}/\text{H}_2\text{O}) = \exp\left(\frac{11.839}{T} - 0.028224\right). \quad (\text{C6})$$

C4 Thermal conductivity

The thermal conductivity of moist air is calculated according to Eqs. (13–16), (13–17) and (13–18) of Pruppacher and Klett (1978) using Mason and Saxena (1958) theory.

For dry air and water vapour, thermal conductivities are, respectively:

$$k_a = 4.3783 \times 10^{-3} + 7.1128 \times 10^{-5}T \text{ J m}^{-1} \text{ s}^{-1} \text{ K}^{-1},$$

$$k_v = -7.0417 \times 10^{-3} + 8.368 \times 10^{-5}T \text{ J m}^{-1} \text{ s}^{-1} \text{ K}^{-1}.$$

The thermal conductivity of moist air is then $k_h = k_a(1 - \gamma_1 - \gamma_2 \frac{k_v}{k_a} \frac{r_v}{r_v + \epsilon})$ with $\gamma_1 = 1.17$ and $\gamma_2 = 1.02$.

Vapour isotopic composition in updrafts

M. Bolot et al.

Title Page

Abstract

Introduction

Conclusions

References

Tables

Figures

◀

▶

◀

▶

Back

Close

Full Screen / Esc

Printer-friendly Version

Interactive Discussion



C5 Molecular diffusivity

The ratio of heavy to light vapour molecular diffusivity in air has been measured by Merlivat (1978) for HDO/H₂O and H₂¹⁸O/H₂O. These measurements have been done at 21 °C and atmospheric pressure in a nitrogen atmosphere, and extended to air using the kinetic theory of gas. The ratios are:

$$K_v/K'_v(\text{HDO}/\text{H}_2\text{O})=1.0251,$$

$$K_v/K'_v(\text{H}_2^{18}\text{O}/\text{H}_2\text{O})=1.0289.$$

The rigid elastic sphere approximation from gas kinetic theory predicts that these ratios are independent of temperature and pressure (Merlivat, 1978).

The molecular diffusivity of light vapour in air has been measured by Hall and Prupacher (1976), yielding $K_v = 0.211 \times 10^{-4} \left(\frac{1013.25}{p} \right) \left(\frac{T}{273.15} \right)^{1.94} \text{ m}^2 \text{ s}^{-1}$ where p is in hPa and T in K.

The diffusivity of water molecules within the crystal lattice of hexagonal ice is about $10^{-14} \text{ m}^2 \text{ s}^{-1}$ (Kuhn and Thürkauf, 1958), and self-diffusivity of liquid water is about $10^{-9} \text{ m}^2 \text{ s}^{-1}$ (Wang, 1951a).

Appendix D

Thermal relaxation and freezing times

The characteristic time of freezing for droplets freely falling in air is given by Johnson and Hallett (1968) as:

$$t_f = \frac{a^2 \rho_l L_f \left(1 - c_l \frac{T^{(\text{eq})} - T}{L_f} \right)}{3k'_{\text{hli}} (T^{(\text{eq})} - T)}, \quad (\text{D1})$$

Vapour isotopic composition in updrafts

M. Bolot et al.

Title Page

Abstract

Introduction

Conclusions

References

Tables

Figures

◀

▶

◀

▶

Back

Close

Full Screen / Esc

Printer-friendly Version

Interactive Discussion



with $k'_{\text{h|l}} = \left(k_{\text{h}} + \frac{L_i K_v}{T} \left(\frac{L_i}{R_v^* T} - 1 \right) \rho_{\text{sat}}^i \right)$, $T^{(\text{eq})} = 0^\circ\text{C}$ is the equilibrium temperature of freezing, and T is air temperature (see Supplement Sect. 2 for a detailed derivation of t_f).

t_f is infinite in the limit $T \rightarrow 0^\circ\text{C}$. However, at small supercoolings $(T^{(\text{eq})} - T)$, other mechanisms extract heat more efficiently than conduction and evaporation to air.

Namely, in the vicinity of the 0°C level, droplets freeze to a large extent by contact with precipitating ice crystals, in which case latent heat extraction happens very fast by conduction through ice. Thus, Eq. (D1) must be considered as a lower bound on the freezing relaxation time, and used to show, when it is smaller than the isotopic relaxation time (see Appendix D), that freezing does not lead to isotopic fractionation.

The definition of thermal relaxation time t_h is provided by Mason (1956) as:

$$t_h = \frac{\rho_{l,i} c_{l,i} a^2}{3k'_{\text{h|l},i}}, \quad (\text{D2})$$

where $k'_{\text{h|l}}$ is defined as $k'_{\text{h|l}}$ but for liquid L_l and ρ_{sat}^l (see Supplement Sect. 2 for a detailed derivation of t_h). One notices from Eq. (D2) that t_h is smaller for ice crystals than for droplets.

Figure B1 compares the homogeneous freezing time of droplets freely suspended in air (Johnson and Hallett, 1968) to isotopic relaxation times. At temperatures below -10°C , estimated freezing times are at least ten times faster than isotopic relaxation times. At temperatures above -10°C , the calculations of Fig. B1 are likely not relevant, since droplets at these temperatures will freeze heterogeneously in accretion processes. The assumption of fast droplet freezing can therefore be safely extended to the whole domain below 0°C in our model.

Supplementary material related to this article is available online at:
<http://www.atmos-chem-phys-discuss.net/12/22451/2012/acpd-12-22451-2012-supplement.pdf>.

22505

ACPD

12, 22451–22533, 2012

Vapour isotopic composition in updrafts

M. Bolot et al.

Title Page

Abstract

Introduction

Conclusions

References

Tables

Figures

◀

▶

◀

▶

Back

Close

Full Screen / Esc

Printer-friendly Version

Interactive Discussion



Acknowledgements. This work was supported in part by grants from INSU and from the NSF International Collaboration in Chemistry (grant # 1026830). M.B. acknowledges fellowships from Ecole Normale Supérieure and Université Pierre et Marie Curie. The authors thank Jim Anderson for hosting M.B. during the initiation of this work and Jean Jouzel and Jun-Ichi Yano for helpful discussions.



The publication of this article is financed by CNRS-INSU.

References

- 10 Bergeron, T.: On the physics of clouds and precipitation, in: Procès Verbaux de l'Association de Météorologie, International Union of Geodesy and Geophysics, 156–178, 1935. 22468
- Berkelhammer, M., Risi, C., Kurita, N., and Noone, D. C.: The moisture source sequence for the Madden-Julian oscillation as derived from satellite retrievals of HDO and H₂O, *J. Geophys. Res.*, 117, D03106, doi:10.1029/2011JD016803, 2012. 22455, 22490
- 15 Bigeleisen, J.: Statistical mechanics of isotope effects on the thermodynamic properties of condensed systems, *J. Chem. Phys.*, 34, 1485–1493, doi:10.1063/1.1701033, 1961. 22457
- Blossey, P. N., Kuang, Z., and Roms, D. M.: Isotopic composition of water in the tropical tropopause layer in cloud-resolving simulations of an idealized tropical circulation, *J. Geophys. Res.*, 115, D24309, doi:10.1029/2010JD014554, 2010. 22453, 22454, 22456, 22483, 22487
- 20 Bony, S., Risi, C., and Vimeux, F.: Influence of convective processes on the isotopic composition ($\delta^{18}\text{O}$ and δD) of precipitation and water vapor in the tropics: 1. Radiative-convective equilibrium and tropical ocean-global atmosphere-coupled ocean-atmosphere

Vapour isotopic composition in updrafts

M. Bolot et al.

Title Page

Abstract

Introduction

Conclusions

References

Tables

Figures

⏪

⏩

◀

▶

Back

Close

Full Screen / Esc

Printer-friendly Version

Interactive Discussion



Vapour isotopic composition in updrafts

M. Bolot et al.

Title Page

Abstract

Introduction

Conclusions

References

Tables

Figures

◀

▶

◀

▶

Back

Close

Full Screen / Esc

Printer-friendly Version

Interactive Discussion



response experiment (TOGA-COARE) simulations, *J. Geophys. Res.*, 113, D19 305, doi:10.1029/2008JD009942, 2008. 22453, 22454, 22487

Botev, Z. I., Grotowski, J. F., and Kroese, D. P.: Kernel density estimation via diffusion, *The Annals of Statistics*, 38, 2916–2957, doi:10.1214/10-AOS799, 2010. 22489

5 Bryan, G. H. and Fritsch, J. M.: A reevaluation of ice–liquid water potential temperature, *Mon. Wea. Rev.*, 132, 2421–2431, doi:10.1175/1520-0493(2004)132<2421:ROIWP>2.0.CO;2, 2004. 22464, 22465

Chapman, S. and Cowling, T. G.: *The Mathematical Theory of Non Uniform Gases*, Cambridge Mathematical Library, Cambridge Univ. Press, Cambridge, UK, 1970. 22498

10 Ciais, P. and Jouzel, J.: Deuterium and oxygen 18 in precipitation: isotopic model, including mixed cloud processes, *J. Geophys. Res.*, 99, 16 793–16 803, doi:10.1029/94JD00412, 1994. 22459, 22482, 22499

Cotton, W. R., Bryan, G. H., and van den Heever, S. C.: *Storm and cloud dynamics*, vol. 99 of *International Geophysics Series*, Academic Press, 2nd Edn., 2011. 22480

15 Couhert, A., Schneider, T., Li, J., Waliser, D. E., and Tompkins, A. M.: The maintenance of the relative humidity of the subtropical free troposphere, *J. Climate*, 23, 390–403, doi:10.1175/2009JCLI2952.1, 2010. 22453

Craig, H.: Isotopic variations in meteoric waters, *Science*, 133, 1702–1703, doi:10.1126/science.133.3465.1702, 1961a. 22484

20 Craig, H.: Standard for reporting concentrations of deuterium and oxygen-18 in natural waters, *Science*, 133, 1833–1834, doi:10.1126/science.133.3467.1833, 1961b. 22485

Craig, H. and Gordon, L. I.: Deuterium and oxygen-18 variations in the ocean and the marine atmosphere, in: *Proceedings of a Conference on Stable Isotopes in Oceanographic Studies and Paleotemperatures*, edited by: Tongiorgi, E., Spoleto, Italy, 9–130, 1965. 22458, 22477

25 Dansgaard, W.: Stable isotops in precipitation, *Tellus*, 16, 436–468, doi:10.1111/j.2153-3490.1964.tb00181.x, 1964. 22452, 22458, 22475, 22478, 22484, 22486

Dee, D. P., Uppala, S. M., Simmons, A. J., Berrisford, P., Poli, P., Kobayashi, S., Andrae, U., Balmaseda, M. A., Balsamo, G., Bauer, P., Bechtold, P., Beljaars, A. C. M., van de Berg, L., Bidlot, J., Bormann, N., Delsol, C., Dragani, R., Fuentes, M., Geer, A. J., Haimberger, L., Healy, S. B., Hersbach, H., Hólm, E. V., Isaksen, I., Kållberg, P., Köhler, M., Matricardi, M., McNally, A. P., Monge-Sanz, B. M., Morcrette, J.-J., Park, B.-K., Peubey, C., de Rosnay, P., Tavolato, C., Thépaut, J.-N., and Vitart, F.: The ERA-Interim reanalysis: configuration

Vapour isotopic composition in updrafts

M. Bolot et al.

Title Page

Abstract

Introduction

Conclusions

References

Tables

Figures

◀

▶

◀

▶

Back

Close

Full Screen / Esc

Printer-friendly Version

Interactive Discussion



and performance of the data assimilation system, Q. J. R. Meteorol. Soc., 137, 553–597, doi:10.1002/qj.828, 2011. 22477, 22516

DePaolo, D. J.: Surface kinetic model for isotopic and trace element fractionation during precipitation of calcite from aqueous solutions, Geochim. Cosmochim. Ac., 75, 1039–1056, 2011. 22462

Federer, B., Brichet, N., and Jouzel, J.: Stable isotopes in hailstones. Part 1: The isotopic cloud model, J. Atmos. Sci., 39, 1323–1335, doi:10.1175/1520-0469(1982)039<1323:SIHPI>2.0.CO;2, 1982. 22454, 22474, 22475, 22477, 22481, 22484

Fierro, A. O., Simpson, J., Lemone, M. A., Straka, J. M., and Smull, B. F.: On how hot towers fuel the hadley cell: an observational and modeling study of line-organized convection in the equatorial trough from TOGA COARE, J. Atmos. Sci., 66, 2730, doi:10.1175/2009JAS3017.1, 2009. 22455

Folkens, I. and Martin, R. V.: The vertical structure of tropical convection and its impact on the budgets of water vapor and ozone, J. Atmos. Sci., 62, 1560–1573, doi:10.1175/JAS3407.1, 2005. 22453

Fudeyasu, H., Ichiyangi, K., Sugimoto, A., Yoshimura, K., Ueta, A., Yamanaka, M. D., and Ozawa, K.: Isotope ratios of precipitation and water vapor observed in Typhoon Shanshan, J. Geophys. Res., 113, D12113, doi:10.1029/2007JD009313, 2008. 22455, 22490

Fueglistaler, S., Dessler, A. E., Dunkerton, T. J., Folkens, I., Fu, Q., and Mote, P. W.: Tropical tropopause layer, Rev. Geophys., 47, G1004+, doi:10.1029/2008RG000267, 2009. 22453

Gedzelman, S. D. and Arnold, R.: Modeling the isotopic composition of precipitation, J. Geophys. Res., 99, 10 455–10 472, doi:10.1029/93JD03518, 1994. 22454, 22456, 22497

Gedzelman, S. D. and Lawrence, J. R.: The isotopic composition of cyclonic precipitation., J. Appl. Meteor., 21, 1385–1404, doi:10.1175/1520-0450(1982)021<1385:TICOCP>2.0.CO;2, 1982. 22458

Gonfiantini, R.: Standards for stable isotope measurements in natural compounds, Nature, 271, 534–536, doi:10.1038/271534a0, 1978. 22456

Hagemann, R., Nief, G., and Roth, E.: Absolute isotopic scale for deuterium analysis of natural waters. Absolute D/H ratio for SMOW, Tellus, 22, 712–715, doi:10.1111/j.2153-3490.1970.tb00540.x, 1970. 22456, 22502

Vapour isotopic composition in updrafts

M. Bolot et al.

Title Page

Abstract

Introduction

Conclusions

References

Tables

Figures

◀

▶

◀

▶

Back

Close

Full Screen / Esc

Printer-friendly Version

Interactive Discussion



- Hall, W. D. and Pruppacher, H. R.: The survival of ice particles falling from cirrus clouds in subsaturated air, *J. Atmos. Sci.*, 33, 1995–2006, doi:10.1175/1520-0469(1976)033<1995:TSOIPF>2.0.CO;2, 1976. 22504
- Hanisco, T. F., Moyer, E. J., Weinstock, E. M., St. Clair, J. M., Sayres, D. S., Smith, J. B., Lockwood, R., Anderson, J. G., Dessler, A. E., Keutsch, F. N., Spackman, J. R., Read, W. G., and Bui, T. P.: Observations of deep convective influence on stratospheric water vapor and its isotopic composition, *Geophys. Res. Lett.*, 34, L04 814, doi:10.1029/2006GL027899, 2007. 22453, 22492
- Herbin, H., Hurtmans, D., Clerbaux, C., Clarisse, L., and Coheur, P.-F.: H_2^{16}O and HDO measurements with IASI/MetOp, *Atmos. Chem. Phys.*, 9, 9433–9447, doi:10.5194/acp-9-9433-2009, 2009. 22492
- Herzfeld, K. F. and Teller, E.: The vapor pressure of isotopes, *Phys. Rev.*, 54, 912–915, doi:10.1103/PhysRev.54.912, 1938. 22457
- Hoffmann, G., Werner, M., and Heimann, M.: Water isotope module of the ECHAM atmospheric general circulation model: a study on timescales from days to several years, *J. Geophys. Res.*, 103, 16 871–16 896, doi:10.1029/98JD00423, 1998. 22479, 22487
- Houze, R. A. J.: *Cloud Dynamics*, vol. 53 of International Geophysics Series, Academic Press, San Diego, 1993. 22463
- Johnson, D. A. and Hallett, J.: Freezing and shattering of supercooled water drops, *Q. J. R. Meteorol. Soc.*, 94, 468–482, doi:10.1002/qj.49709440204, 1968. 22504, 22505
- Joussaume, S., Sadourny, R., and Jouzel, J.: A general circulation model of water isotope cycles in the atmosphere, *Nature*, 311, 24–29, doi:10.1038/311024a0, 1984. 22453
- Jouzel, J. and Merlivat, L.: Deuterium and oxygen 18 in precipitation: modeling of the isotopic effects during snow formation, *J. Geophys. Res.*, 89, 11 749–11 758, doi:10.1029/JD089iD07p11749, 1984. 22453, 22456, 22458, 22459, 22478, 22479, 22499, 22501
- Jouzel, J., Merlivat, L., and Roth, E.: Isotopic study of hail, *J. Geophys. Res.*, 80, 5015–5030, doi:10.1029/JC080i036p05015, 1975. 22453, 22454, 22456, 22475, 22497, 22498, 22499
- Kirkpatrick, C., McCaul, E. W., and Cohen, C.: Variability of updraft and downdraft characteristics in a large parameter space study of convective storms, *Mon. Wea. Rev.*, 137, 1550, doi:10.1175/2008MWR2703.1, 2009. 22455
- Korolev, A. V.: Limitations of the Wegener Bergeron Findeisen mechanism in the evolution of mixed-phase clouds, *J. Atmos. Sci.*, 64, 3372–3375, doi:10.1175/JAS4035.1, 2007. 22468

- Korolev, A. V. and Mazin, I. P.: Supersaturation of water vapor in clouds, *J. Atmos. Sci.*, 60, 2957–2974, doi:10.1175/1520-0469(2003)060<2957:SOWVIC>2.0.CO;2, 2003. 22458, 22466, 22467, 22479
- 5 Kuang, Z., Toon, G. C., Wennberg, P. O., and Yung, Y. L.: Measured HDO/H₂O ratios across the tropical tropopause, *Geophys. Res. Lett.*, 30, 1372, doi:10.1029/2003GL017023, 2003. 22453
- Kuhn, W. and Thürkauf, M.: Isotopentrennung beim Gefrieren von Wasser und Diffusionskonstanten von D und ¹⁸O im Eis. Mit Diskussion der Möglichkeit einer Multiplikation der beim Gefrieren auftretenden Isotopentrennung in einer Haarnadelgegenstromvorrichtung, *Helv. Chim. Acta*, 41, 938–971, doi:10.1002/hlca.19580410408, 1958. 22500, 22504
- 10 Kurita, N., Noone, D., Risi, C., Schmidt, G. A., Yamada, H., and Yoneyama, K.: Intraseasonal isotopic variation associated with the Madden-Julian oscillation, *J. Geophys. Res.*, 116, D24101, doi:10.1029/2010JD015209, 2011. 22453, 22455, 22479, 22487, 22490
- Kuroda, T.: Rate determining processes of growth of ice crystals from the vapour phase. I: Theoretical consideration, *J. Meteor. Soc. Japan*, 62, 552–562, 1984. 22462
- 15 Kursinski, E. R., Feng, D., Flittner, D., Hajj, G., Herman, B., Romberg, F., Syndergaard, S., Ward, D., and Yunck, T.: An active microwave limb sounder for profiling water vapour, ozone, temperature, geopotential, clouds, isotopes and stratospheric winds, in: *Occultations for Probing Atmosphere and Climate (OPAC-1)*, Springer-Verlag, Berlin, 2004. 22492
- 20 Lanotte, A. S., Seminara, A., and Toschi, F.: Cloud droplet growth by condensation in homogeneous isotropic turbulence, *J. Atmos. Sci.*, 66, 1685–1697, doi:10.1175/2008JAS2864.1, 2009. 22493
- Lawrence, J. R. and Gedzelman, S. D.: Low stable isotope ratios of tropical cyclone rains, *Geophys. Res. Lett.*, 23, 527–530, doi:10.1029/96GL00425, 1996. 22455, 22490
- 25 Lawrence, J. R. and Gedzelman, S. D.: Tropical ice core isotopes: do they reflect changes in storm activity?, *Geophys. Res. Lett.*, 30, 1072, doi:10.1029/2002GL015906, 2003. 22455, 22490
- Lawrence, J. R., Gedzelman, S. D., Dexheimer, D., Cho, H., Carrie, G. D., Gasparini, R., Anderson, C. R., Bowman, K. P., and Biggerstaff, M. I.: Stable isotopic composition of water vapor in the tropics, *J. Geophys. Res.*, 109, D06 115, doi:10.1029/2003JD004046, 2004. 22477
- 30 Lawson, R. P., Jensen, E., Mitchell, D. L., Baker, B., Mo, Q., and Pilson, B.: Microphysical and radiative properties of tropical clouds investigated in TC4 and NAMMA, *J. Geophys. Res.*, 115, D00J08, doi:10.1029/2009JD013017, 2010. 22479

Vapour isotopic composition in updrafts

M. Bolot et al.

Title Page

Abstract

Introduction

Conclusions

References

Tables

Figures

◀

▶

◀

▶

Back

Close

Full Screen / Esc

Printer-friendly Version

Interactive Discussion



Vapour isotopic composition in updrafts

M. Bolot et al.

[Title Page](#)[Abstract](#)[Introduction](#)[Conclusions](#)[References](#)[Tables](#)[Figures](#)[◀](#)[▶](#)[◀](#)[▶](#)[Back](#)[Close](#)[Full Screen / Esc](#)[Printer-friendly Version](#)[Interactive Discussion](#)

- Lee, J.-E., Fung, I., DePaolo, D. J., and Henning, C. C.: Analysis of the global distribution of water isotopes using the NCAR atmospheric general circulation model, *J. Geophys. Res.*, 112, D16306, doi:10.1029/2006JD007657, 2007. 22479, 22487
- Lee, J.-E., Pierrehumbert, R., Swann, A., and Lintner, B. R.: Sensitivity of stable water isotopic values to convective parameterization schemes, *Geophys. Res. Lett.*, 362, L23801, doi:10.1029/2009GL040880, 2009. 22453, 22454
- LeMone, M. A. and Zipser, E. J.: Cumulonimbus vertical velocity events in GATE. Part 1: Diameter, intensity and mass flux, *J. Atmos. Sci.*, 37, 2444–2457, doi:10.1175/1520-0469(1980)037<2444:CVVEIG>2.0.CO;2, 1980. 22455
- Majoube, M.: Fractionation factor of ^{18}O between water vapour and ice, *Nature*, 226, 1242, doi:10.1038/2261242a0, 1970. 22503
- Majoube, M.: Fractionnement en oxygène 18 et en deutérium entre l'eau et sa vapeur., *J. Chim. Phys. Physicochim. Biol.*, 10, 1423–1436, 1971. 22503
- Mason, B. J.: On the melting of hailstones, *Q. J. R. Meteorol. Soc.*, 82, 209–216, doi:10.1002/qj.49708235207, 1956. 22494, 22505
- Mason, B. J.: *The Physics of Clouds*, Oxford Monogr. Meteorol., Clarendon, Oxford, 1971. 22495
- Mason, E. A. and Saxena, S. C.: Approximate formula for the thermal conductivity of gas mixtures, *Phys. Fluids*, 1, 361–369, doi:10.1063/1.1724352, 1958. 22503
- Merlivat, L.: Molecular diffusivities of H_2^{16}O , HD^{16}O , and H_2^{18}O in gases, *J. Chem. Phys.*, 69, 2864–2871, doi:10.1063/1.436884, 1978. 22458, 22504
- Merlivat, L. and Jouzel, J.: Global climatic interpretation of the deuterium-oxygen 18 relationship for precipitation, *J. Geophys. Res.*, 84, 5029–5033, doi:10.1029/JC084iC08p05029, 1979. 22484
- Merlivat, L. and Nief, G.: Fractionnement isotopique lors des changements d'état solide-vapeur et liquide-vapeur de l'eau à des températures inférieures à 0°C , *Tellus*, 19, 122–127, doi:10.1111/j.2153-3490.1967.tb01465.x, 1967. 22503
- Moyer, E. J., Irion, F. W., Yung, Y. L., and Gunson, M. R.: ATMOS stratospheric deuterated water and implications for troposphere-stratosphere transport, *Geophys. Res. Lett.*, 23, 2385–2388, doi:10.1029/96GL01489, 1996. 22453, 22454, 22475, 22477, 22478, 22481, 22482
- Murphy, D. M. and Koop, T.: Revue of the vapour pressures of ice and supercooled water for atmospheric applications, *Q. J. R. Meteorol. Soc.*, 131, 1539–1565, doi:10.1256/qj.04.94, 2005. 22502

Vapour isotopic composition in updrafts

M. Bolot et al.

Title Page

Abstract

Introduction

Conclusions

References

Tables

Figures

◀

▶

◀

▶

Back

Close

Full Screen / Esc

Printer-friendly Version

Interactive Discussion



- Nassar, R., Bernath, P. F., Boone, C. D., Gettelman, A., McLeod, S. D., and Rinsland, C. P.: Variability in HDO/H₂O abundance ratios in the tropical tropopause layer, *J. Geophys. Res.*, 112, D21 305, doi:10.1029/2007JD008417, 2007. 22453, 22454, 22492
- 5 Nelson, J.: Theory of isotopic fractionation on faceted ice crystals, *Atmos. Chem. Phys.*, 11, 11351–11360, doi:10.5194/acp-11-11351-2011, 2011. 22462
- Orville, H. D. and Kopp, F. J.: Numerical simulation of the life history of a hailstorm., *J. Atmos. Sci.*, 34, 1596–1618, doi:10.1175/1520-0469(1977)034<1596:NSOTLH>2.0.CO;2, 1977. 22483
- 10 Pierrehumbert, R. T. and Roca, R.: Evidence for control of atlantic subtropical humidity by large scale advection, *Geophys. Res. Lett.*, 25, 4537–4540, doi:10.1029/1998GL900203, 1998. 22453
- Pruppacher, H. R. and Klett, J. D.: *Microphysics of Clouds and Precipitation*, D. Reidel, Norwell, Mass. USA, 1978. 22492, 22503
- 15 Randel, W. J., Moyer, E., Park, M., Jensen, E., Bernath, P., Walker, K., and Boone, C.: Global variations of HDO and HDO/H₂O ratios in the upper troposphere and lower stratosphere derived from ACE-FTS satellite measurements, *J. Geophys. Res.*, 117, D06303, doi:10.1029/2011JD016632, 2012. 22454, 22492
- Rayleigh, L. and Ramsay, W.: Argon, a new constituent of the atmosphere, *Phil. Trans. R. Soc. Lond. A*, 186, 187–241, doi:10.1098/rsta.1895.0006, 1895. 22475
- 20 Riehl, H. and Malkus, J. S.: On the heat balance in the equatorial trough zone, *Geophysica*, 6, 503–537, 1958. 22455
- Risi, C., Bony, S., Vimeux, F., Descroix, L., Ibrahim, B., Lebreton, E., Mamadou, I., and Sultan, B.: What controls the isotopic composition of the African monsoon precipitation? Insights from event-based precipitation collected during the 2006 AMMA field campaign, *Geophys. Res. Lett.*, 35, L24 808, doi:10.1029/2008GL035920, 2008. 22453, 22490
- 25 Risi, C., Bony, S., Vimeux, F., and Jouzel, J.: Water-stable isotopes in the LMDZ4 general circulation model: model evaluation for present-day and past climates and applications to climatic interpretations of tropical isotopic records, *J. Geophys. Res.*, 115, D12118, doi:10.1029/2009JD013255, 2010. 22479, 22487
- 30 Risi, C., Noone, D., Worden, J., Frankenberg, C., Stiller, G., Kiefer, M., Funke, B., Walker, K., Bernath, P., Schneider, M., Bony, S., Lee, J., Brown, D., and Sturm, C.: Process-evaluation of tropospheric humidity simulated by general circulation models using water vapor isotopic observations: 2. Using isotopic diagnostics to understand the mid and upper

Vapour isotopic composition in updrafts

M. Bolot et al.

Title Page

Abstract

Introduction

Conclusions

References

Tables

Figures

◀

▶

◀

▶

Back

Close

Full Screen / Esc

Printer-friendly Version

Interactive Discussion



tropospheric moist bias in the tropics and subtropics, *J. Geophys. Res.*, 117, D05304, doi:10.1029/2011JD016623, 2012. 22453, 22479

Rosenfeld, D. and Woodley, W. L.: Deep convective clouds with sustained supercooled liquid water down to -37.5°C , *Nature*, 405, 440–442, doi:10.1038/35013030, 2000. 22480

5 Sayres, D. S., Moyer, E. J., Hanisco, T. F., St. Clair, J. M., Keutsch, F. N., O'Brien, A., Allen, N. T., Lapson, L., Demusz, J. N., Rivero, M., Martin, T., Greenberg, M., Tuozzolo, C., Engel, G. S., Kroll, J. H., Paul, J. B., and Anderson, J. G.: A new cavity based absorption instrument for detection of water isotopologues in the upper troposphere and lower stratosphere, *Rev. of Sci. Inst.*, 80, 044102, doi:10.1063/1.3117349, 2009. 22454

10 Sayres, D. S., Pfister, L., Hanisco, T. F., Moyer, E. J., Smith, J. B., St. Clair, J. M., O'Brien, A. S., Witinski, M. F., Legg, M., and Anderson, J. G.: Influence of convection on the water isotopic composition of the tropical tropopause layer and tropical stratosphere, *J. Geophys. Res.*, 115, D00J20, doi:10.1029/2009JD013100, 2010. 22453, 22492

15 Schmidt, G. A., Hoffmann, G., Shindell, D. T., and Hu, Y.: Modeling atmospheric stable water isotopes and the potential for constraining cloud processes and stratosphere-troposphere water exchange, *J. Geophys. Res.*, 110, D21 314, doi:10.1029/2005JD005790, 2005. 22453

Schmidt, G. A., LeGrande, A. N., and Hoffmann, G.: Water isotope expressions of intrinsic and forced variability in a coupled ocean-atmosphere model, *J. Geophys. Res.*, 112, D10103, doi:10.1029/2006JD007781, 2007. 22479, 22487

20 Smith, J. A., Ackerman, A. S., Jensen, E. J., and Toon, O. B.: Role of deep convection in establishing the isotopic composition of water vapor in the tropical transition layer, *Geophys. Res. Lett.*, 330, L06 812, doi:10.1029/2005GL024078, 2006. 22453

Squires, P.: The growth of cloud drops by condensation. I. General characteristics, *Aust. J. Sci. Res. A*, 5, 59–86, 1952. 22479

25 Steinwagner, J., Milz, M., von Clarmann, T., Glatthor, N., Grabowski, U., Höpfner, M., Stiller, G. P., and Röckmann, T.: HDO measurements with MIPAS, *Atmos. Chem. Phys.*, 7, 2601–2615, doi:10.5194/acp-7-2601-2007, 2007. 22453, 22454

Stewart, M. K.: Stable isotope fractionation due to evaporation and isotopic exchange of falling waterdrops: applications to atmospheric processes and evaporation of lakes, *J. Geophys. Res.*, 80, 1133–1146, doi:10.1029/JC080i009p01133, 1975. 22498

30 Stichler, W., Gonfiantini, R., and Rozanski, K.: Reference and intercomparison materials for stable isotopes of light elements, IAEA-TECDOC 825, IAEA, Vienna, Austria, 1995. 22456

- Stith, J. L., Dye, J. E., Bansemer, A., Heymsfield, A. J., Grainger, C. A., Petersen, W. A., and Cifelli, R.: Microphysical observations of tropical clouds, *J. Appl. Meteorol.*, 41, 97–117, doi:10.1175/1520-0450(2002)041<0097:MOOTC>2.0.CO;2, 2002. 22479
- Stith, J. L., Haggerty, J. A., Heymsfield, A., and Grainger, C. A.: Microphysical characteristics of tropical updrafts in clean conditions, *J. Appl. Meteorol.*, 43, 779–794, doi:10.1175/2104.1, 2004. 22480
- Tindall, J. C., Valdes, P. J., and Sime, L. C.: Stable water isotopes in HadCM3: isotopic signature of El Niño-Southern Oscillation and the tropical amount effect, *J. Geophys. Res.*, 114, D04111, doi:10.1029/2008JD010825, 2009. 22479, 22487
- Tripoli, G. J. and Cotton, W. R.: The use of ice-liquid water potential temperature as a thermodynamic variable in deep atmospheric models, *Mon. Wea. Rev.*, 109, 1094–1102, doi:10.1175/1520-0493(1981)109<1094:TUOLLW>2.0.CO;2, 1981. 22464
- Twomey, S.: The nuclei of natural cloud formation. Part II: The supersaturation in natural clouds and the variation of cloud droplet concentration, *Geophys. Pura e Appl.*, 43, 243–249, 1959. 22479
- Urey, H.: The thermodynamics of isotopic substances, *J. Chem. Soc.*, 1947, 562–581, doi:10.1039/JR9470000562, 1947. 22457
- Van Hook, W. A.: Vapor pressures of the isotopic waters and ices, *J. Phys. Chem.*, 72, 1234–1244, doi:10.1021/j100850a028, 1968. 22457
- Wang, J. H.: Self-diffusion and structure of liquid water. I. Measurement of self-diffusion of liquid water with deuterium as tracer, *J. Amer. Chem. Soc.*, 73, 510–513, doi:10.1021/ja01146a002, 1951a. 22504
- Wang, J. H.: Self-diffusion and structure of liquid water. II. Measurement of self-diffusion of liquid water with ^{18}O as tracer, *J. Amer. Chem. Soc.*, 73, 4181–4183, doi:10.1021/ja01153a039, 1951b. 22497
- Warner, J.: The supersaturation in natural clouds, *J. Rech. Atmos.*, 3, 233–237, 1968. 22466
- Wegener, A.: *Thermodynamik der Atmosphäre*, J. A. Barth, Leipzig, 1911. 22468
- Worden, J., Noone, D., Galewsky, J., Bailey, A., Bowman, K., Brown, D., Hurley, J., Kulawik, S., Lee, J., and Strong, M.: Estimate of bias in Aura TES HDO/H₂O profiles from comparison of TES and in situ HDO/H₂O measurements at the Mauna Loa observatory, *Atmos. Chem. Phys.*, 11, 4491–4503, doi:10.5194/acp-11-4491-2011, 2011. 22453

Vapour isotopic composition in updrafts

M. Bolot et al.

[Title Page](#)[Abstract](#)[Introduction](#)[Conclusions](#)[References](#)[Tables](#)[Figures](#)[⏪](#)[⏩](#)[◀](#)[▶](#)[Back](#)[Close](#)[Full Screen / Esc](#)[Printer-friendly Version](#)[Interactive Discussion](#)

Wright, J. S., Sobel, A. H., and Schmidt, G. A.: Influence of condensate evaporation on water vapor and its stable isotopes in a GCM, *Geophys. Res. Lett.*, 361, L12804, doi:10.1029/2009GL038091, 2009. 22453

5 Yoshimura, K., Kanamitsu, M., Noone, D., and Oki, T.: Historical isotope simulation using reanalysis atmospheric data, *J. Geophys. Res.*, 113, D19108, doi:10.1029/2008JD010074, 2008. 22479, 22487

Vapour isotopic composition in updrafts

M. Bolot et al.

Title Page

Abstract

Introduction

Conclusions

References

Tables

Figures

⏪

⏩

◀

▶

Back

Close

Full Screen / Esc

Printer-friendly Version

Interactive Discussion



Vapour isotopic composition in updrafts

M. Bolot et al.

Table 1. Relation between internal parameters ζ , γ and C_1 of the model and physical quantities. Rows 1 and 2: vapour saturation over ice at $T \leq -40^\circ\text{C}$ as a function of ζ obtained from Eq. (6). Rows 3 to 9: glaciation temperature, altitude and pressure as a function of γ for two extreme values of the auto-conversion coefficient for liquid water C_1 . Temperature is computed from a full integration of the model with cloud base level at 1050 m. Pressure and altitude grids come from a mean tropical profile from the ERA-Interim reanalysis (Dee et al., 2011). The saturation parameter ζ is set to 1 in these computations. Setting it to 0 affects the glaciation temperature by less than 3% in all cases. Rows 10 and 11: ratio $r_1/r_{1,\text{adiab}}$ at $T = 0^\circ\text{C}$ between the (active) liquid water content for a given value of C_1 and the same quantity for $C_1 = 0$ (adiabatic content). This ratio is calculated from a full integration of the model and is not sensitive to glaciation and saturation parameters which are ineffective at positive temperatures.

saturation parameter ζ		0	0.2	0.4	0.6	0.8	1
S_i at $T < -40^\circ\text{C}$		1	1.09	1.18	1.28	1.37	1.47
glaciation parameter γ		1	2	3	4	6	9
$C_1 = 0$	T_g ($^\circ\text{C}$)	-12.81	-22.74	-28.68	-32.24	-35.93	-38.04
	z_g (km)	7.65	9.15	9.95	10.40	10.85	11.1
	ρ_g (hPa)	396	323	288	270	253	244
$C_1 = 0.5\text{km}^{-1}$	T_g ($^\circ\text{C}$)	-10.71	-18.93	-24.55	-27.93	-32.26	-35.14
	z_g (km)	7.30	8.60	9.40	9.85	10.40	10.75
	ρ_g (hPa)	415	348	312	293	270	257
auto-conversion coefficient C_1		0	0.1	0.2	0.3	0.4	0.5
$r_1/r_{1,\text{adiab}}$ at $T = 0^\circ\text{C}$ (%)		100	80	64	51	40	31

[Title Page](#)
[Abstract](#)
[Introduction](#)
[Conclusions](#)
[References](#)
[Tables](#)
[Figures](#)
[Back](#)
[Close](#)
[Full Screen / Esc](#)
[Printer-friendly Version](#)
[Interactive Discussion](#)


Table 2. Table of symbols used in the text. Some symbols which are only local to a single formula are not listed here. In the last column, suppl stands for the Supplement.

Symbol	Unit	Meaning	Defined near Eq.
a	m	Radius of a droplet	(B3)
A_l, A_i	–	Thermal transfer coefficient between water vapour and condensates (liquid and ice)	(A5)
b	–	Fraction of liquid to ice conversion occurring via the WBF process	(27)
c_{pv}, c_l, c_i	$\text{J kg}^{-1} \text{K}^{-1}$	Specific thermal capacity at constant pressure of water vapour, liquid water and ice	
C	m	Crystal capacitance (effective radius for diffusional growth)	(A1)
$C_{l,i}$	m^{-1}	Auto-conversion coefficients for liquid water and ice	(15)
$e_{\text{sat}}^l, e_{\text{sat}}^i$	Pa	Saturation pressure of water vapour over liquid water and ice	(6), (C1), (C2)
e_{adj}	Pa	Adjusted saturation vapour pressure	(6)
f_h	–	Thermal ventilation coefficient	(A2)
f_v, f'_v	–	Ventilation coefficient for light and heavy isotopologue vapour	(A1), (B1)
k_h	$\text{J m}^{-1} \text{K}^{-1} \text{s}^{-1}$	Thermal conductivity of air	(A2), Sect. C4
$k'_{h ,i}$	$\text{J m}^{-1} \text{K}^{-1} \text{s}^{-1}$	Modified thermal conductivity of air	suppl (4–7)
K_h	$\text{m}^2 \text{s}^{-1}$	Thermal diffusivity of air	(A7)

Vapour isotopic composition in updrafts

M. Bolot et al.

Title Page

Abstract

Introduction

Conclusions

References

Tables

Figures

◀

▶

◀

▶

Back

Close

Full Screen / Esc

Printer-friendly Version

Interactive Discussion



Table 2. Continued.

Symbol	Unit	Meaning	Defined near Eq.
Le	–	Lewis number	(A6), suppl (1)
K_v, K'_v	$\text{m}^2 \text{s}^{-1}$	Molecular diffusivity of light and heavy isotopologue vapour in air	(A1), (B1), Sect. C5
L_l, L_i, L_f	J kg^{-1}	Latent heat of evaporation, sublimation and fusion	Sect. C1
m, m'	kg	Light and heavy isotopologues mass in a single droplet or crystal	(A1), (B1)
p	Pa	Air pressure	
Pr	–	Prandtl number	suppl (Sect. 1)
$q_{\text{sat}}^{\text{l,i}}$	–	Saturation specific humidity with respect to liquid water or ice	(A7)
r_v, r_l, r_i	kg kg^{-1}	Mass mixing ratio of light isotopologue vapour, liquid water and ice	
r'_v, r'_l, r'_i	kg kg^{-1}	Mass mixing ratio of heavy isotopologue vapour, liquid water and ice	
r_t, r'_t	kg kg^{-1}	Total mass mixing ratio of light water and heavy isotopologues	
r_{adj}	kg kg^{-1}	Adjusted mass mixing ratio of water vapour	(6)
R_d^*, R_v^*	$\text{J kg}^{-1} \text{K}^{-1}$	Gas constant for dry air and water vapour	
Re	–	Reynolds number	suppl (Sect. 1)
R_v, R_l, R_i	–	Isotopic ratio of vapour, liquid water or ice	

Vapour isotopic composition in updrafts

M. Bolot et al.

Title Page

Abstract

Introduction

Conclusions

References

Tables

Figures

◀

▶

◀

▶

Back

Close

Full Screen / Esc

Printer-friendly Version

Interactive Discussion



Table 2. Continued.

Symbol	Unit	Meaning	Defined near Eq.
R_0	–	Isotopic ratio of the Vienna Sea Mean Oceanic Water standard	
S_c	–	Schmidt number	suppl (Sect. 1)
S_l, S_i	–	Vapour saturation over liquid water or ice	
$S_l^{(eff)}, S_i^{(eff)}$	–	Effective vapour saturation over liquid water or ice, computed at droplet or ice surface temperature	(1)
t_f	s	Freezing time	(D1)
t_h	s	Thermal relaxation time	(D2)
T	K	Air temperature	
U_∞	ms^{-1}	Particle terminal fall speed	suppl (Sect. 1)
w_{up}	ms^{-1}	Updraft vertical speed	
$X^{(\infty)}$		Value of quantity X in the environment, beyond the boundary layer surrounding droplets or crystals	
$X^{(s)}$		Value of quantity X at the surface of droplets or crystals	
$X^{(p)}$		Value of quantity X for deactivated/precipitated species	
z	m	Altitude	
α_l, α_i	–	Equilibrium fractionation factor for liquid-vapour and ice-vapour phase transition	(C3–C6)

Vapour isotopic composition in updrafts

M. Bolot et al.

Title Page

Abstract

Introduction

Conclusions

References

Tables

Figures

◀

▶

◀

▶

Back

Close

Full Screen / Esc

Printer-friendly Version

Interactive Discussion



Table 2. Continued.

Symbol	Unit	Meaning	Defined near Eq.
α_{kl}, α_{ki}	–	Kinetic fractionation factor for liquid-vapour and ice-vapour phase transition	(1)
$\beta_{i,l}$	–	$\alpha_{i,l}(K_v/K'_v)(f_v/f'_v)$	(1)
γ	–	Glaciation parameter	(11)
$\delta D, \delta^{18}O$	‰	Isotopic depletion in deuterium and oxygen-18	Sect. 2
ϵ	–	R_d^*/R_v^*	
ζ	–	Saturation parameter	(6)
η	–	WBF parameter	(28)
θ_{il}	K	Ice liquid water potential temperature	(5)
Λ	–	Generalised fractionation factor	(30)
μ	Pas	Dynamic viscosity	suppl (Sect. 1)
ξ_i	–	Fraction of condensate growth corresponding to ice deposition	(8)
ρ_{ice}	kgm ⁻³	Density of ice	(C2)
ρ_X	kgm ⁻³	Density of specie X	
ρ_{drop}	kgm ⁻³	Density of a droplet	(B5)
ρ_v, ρ'_v	kgm ⁻³	Density of light water vapour and heavy isotopologue vapour	
$\rho_{sat}^l, \rho_{sat}^i$	kgm ⁻³	Saturation density of water vapour over liquid water and ice	
τ_{drop}	s	E-folding time of droplet isotopic relaxation	(B5)
$\varphi(T)$	–	Fractional conversion rate from liquid water to ice	(11)

Vapour isotopic composition in updrafts

M. Bolot et al.

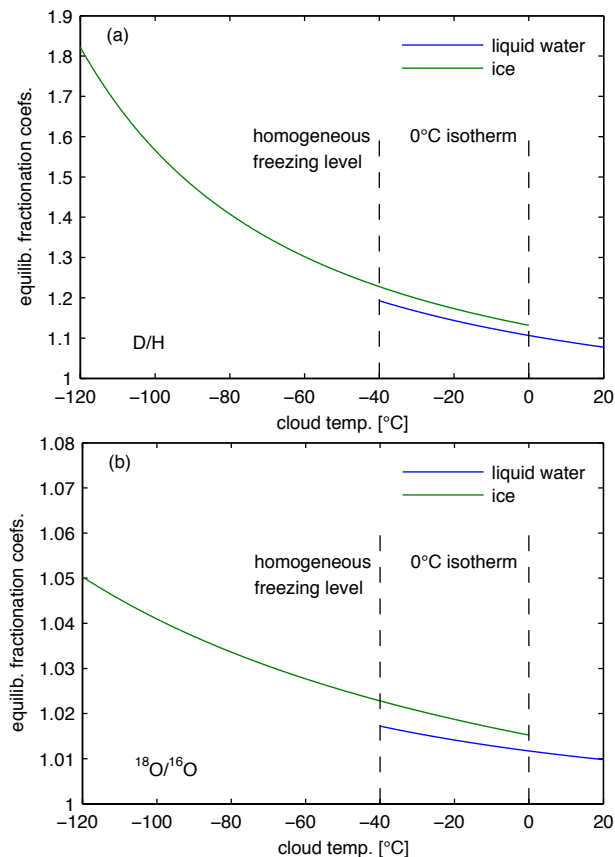


Fig. 1. Equilibrium fractionation factors for vapour-liquid (blue) and vapour-ice (green) phase transition as a function of temperature. **(a)** HDO/H₂O. **(b)** H₂¹⁸O/H₂O. Notice that fractionation over ice is higher than fractionation over liquid in the mixed phase zone. This equilibrium behaviour is eventually reversed when kinetic effects and droplet evaporation are considered (WBF process).

[Title Page](#)
[Abstract](#)
[Introduction](#)
[Conclusions](#)
[References](#)
[Tables](#)
[Figures](#)
[◀](#)
[▶](#)
[◀](#)
[▶](#)
[Back](#)
[Close](#)
[Full Screen / Esc](#)
[Printer-friendly Version](#)
[Interactive Discussion](#)


Vapour isotopic composition in updrafts

M. Bolot et al.

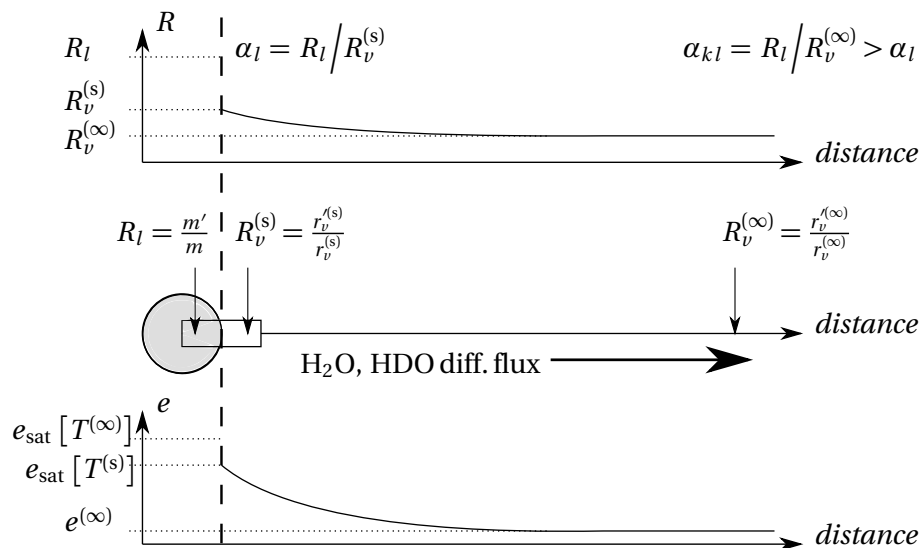


Fig. 2. Sketch of the evaporation of a droplet in a subsaturated environment. The lower panel displays the radial variation of water vapour partial pressure. The upper panel displays the radial variation of vapour isotopic ratios. The superscripts (s) and (∞) denote values at droplet surface and outside the diffusive boundary layer, respectively. Vapour partial pressure decreases across the boundary layer in a way that depends on thermal and molecular diffusivity. Note that $e_{\text{sat}}[T^{(s)}] < e_{\text{sat}}[T^{(\infty)}]$ since the droplet surface is cooled below environmental temperature at evaporation ($e_{\text{sat}} = \text{liquid saturation here}$). Thus, thermal impedance limits subsaturation at droplet surface compared to what it would be if $T^{(s)}$ were equal to $T^{(\infty)}$, and consequently limits isotopic kinetic effects. The decrease of vapour isotopic ratio across the boundary layer explains why the kinetic fractionation factor is enhanced over its equilibrium value. Note also that the whole droplet is assumed to equilibrate with its surrounding (grey shaded area = water actively exchanging with vapour) if its isotopic relaxation time is sufficiently small.

[Title Page](#)
[Abstract](#)
[Introduction](#)
[Conclusions](#)
[References](#)
[Tables](#)
[Figures](#)
[Back](#)
[Close](#)
[Full Screen / Esc](#)
[Printer-friendly Version](#)
[Interactive Discussion](#)

Vapour isotopic composition in updrafts

M. Bolot et al.

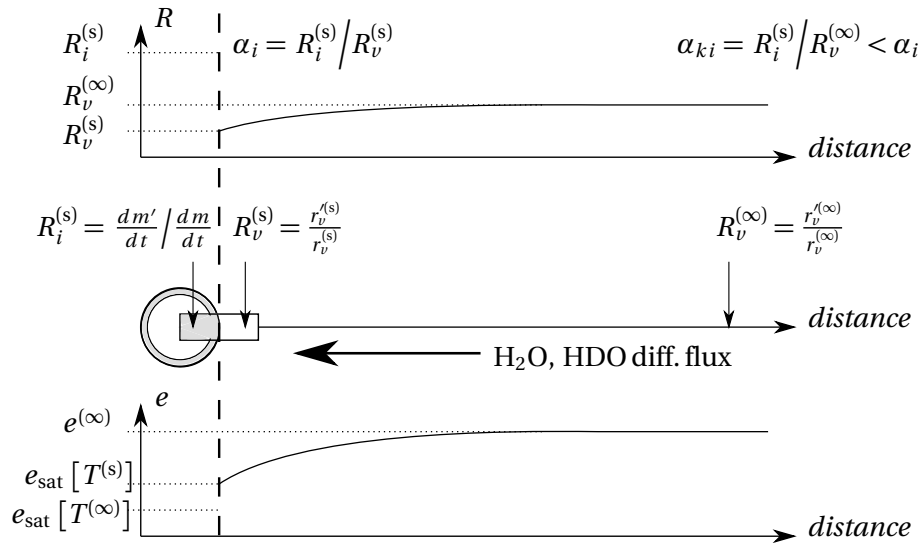


Fig. 3. Same as Fig. 2 but for ice deposition in a supersaturated environment. Vapour pressure is now increasing across the diffusive boundary layer surrounding the crystal, and $e_{\text{sat}}[T^{(s)}] > e_{\text{sat}}[T^{(\infty)}]$ owing to the surface being heated above environmental temperature at deposition (e_{sat} = ice saturation here). Thus thermal impedance reduces supersaturation compared to what it would be if $T^{(s)}$ were equal to $T^{(\infty)}$, and limits kinetic effects at deposition too. The increase of vapour isotopic ratio across the boundary layer explains why the kinetic fractionation factor is reduced compared to its equilibrium value. Note that isotopic equilibration with vapour is restricted to the surface layer of the crystal (grey shaded area). This is the main difference with the droplet case.

Vapour isotopic composition in updrafts

M. Bolot et al.

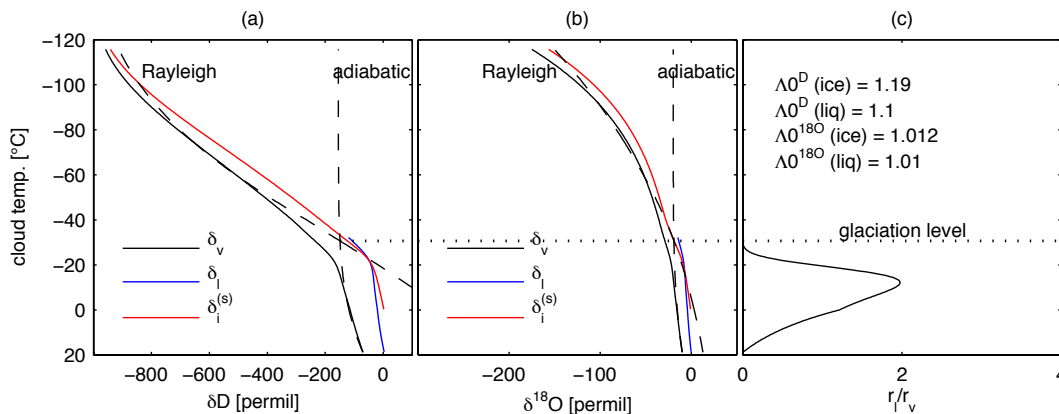


Fig. 4. (a and b) isotopic depletion of water vapour (solid black), (active) liquid water (solid blue) and ice surface layer (solid red) as a function of the temperature of a rising cloud parcel, computed from integrating Eq. (29), compared to the simplified adiabatic and Rayleigh solutions under constant generalised fractionation coefficient Λ_0 (dashed). The integration of Eq. (29) is performed as described in the default scenario of Sect. 4 and the values of Λ_0 for the simplified laws of Eqs. (31) (adiabatic) and (32) (Rayleigh) are given in the right panel. (a) is for HDO/H₂O and (b) is for H₂¹⁸O/H₂O. (c) Ratio of the (active) liquid to vapour mass mixing ratios r_l/r_v . The glaciation level is defined where r_l drops below 10^{-6} kg kg⁻¹. (a, b) The isotopic ratio of active liquid water is computed as $R_l = \alpha_{kl}R_v$, and that of ice surface layer is computed as $R_i^{(s)} = \alpha_{ki}R_v$ (δ_l and δ_i are the corresponding values in δ -notation). Note that the transition from adiabatic to Rayleigh behaviour is less pronounced for oxygen 18 owing to smaller overall fractionation between vapour and condensed phase (the relative mass difference between isotopologues is smaller).

Title Page

Abstract Introduction

Conclusions References

Tables Figures

◀ ▶

◀ ▶

Back Close

Full Screen / Esc

Printer-friendly Version

Interactive Discussion



Vapour isotopic composition in updrafts

M. Bolot et al.

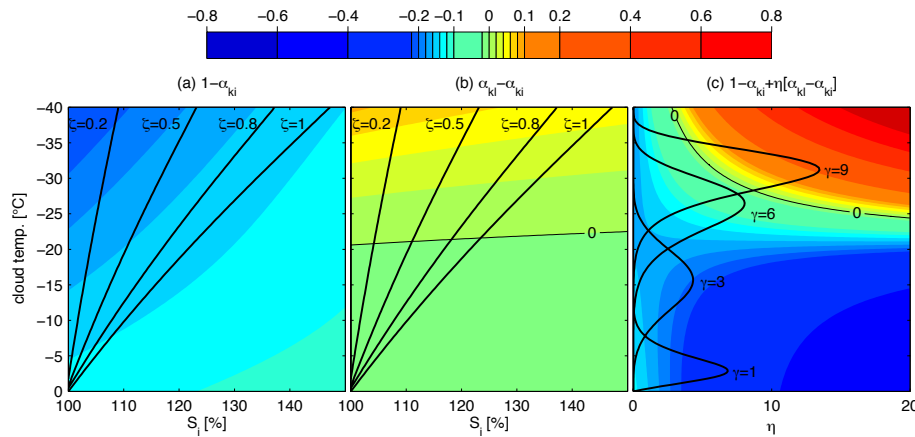


Fig. 5. Variations in the mixed phase domain of $1 - \Lambda = 1 - \alpha_{ki} + \eta(\alpha_{kl} - \alpha_{ki})$ and its components for the HDO/H₂O system (Λ = generalised fractionation factor). ξ_i has been set to 1, in coherence with the discussion in Sect. 4.3. **(a)** Sensitivity to saturation of $1 - \alpha_{ki}$ (corresponding to net adiabatic cooling of moisture). **(b)** Sensitivity to saturation of $\alpha_{kl} - \alpha_{ki}$ (corresponding to droplet evaporation). The line in solid black marks the sign reversal. **(a, b)** Iso- ζ lines correspond to supersaturation over ice for each value of ζ , as computed in the model. **(c)** Sensitivity of $1 - \Lambda$ to the WBF parameter η . ζ has been set to 1. η measures the ratio of the source of vapour from droplet evaporation to that from net adiabatic cooling of moisture. Iso- γ curves show the variations of η for a rising cloud parcel as computed in the model for each value of the glaciation parameter γ . η peaks at some cloud temperature which is somewhat higher than glaciation temperature. This is due to enhanced conversion of liquid to ice near glaciation, while evaporation eventually tails off as liquid water becomes depleted. For $\gamma = 1$ and 3, the WBF process reinforces depletion. For $\gamma = 6$, the WBF process enriches vapour with HDO so that the depletion is decreased compared to the case $\eta = 0$. For $\gamma = 9$, the WBF effect is strong enough to exceed the effect of net adiabatic moisture cooling and the overall effect is vapour enrichment in the range -30°C to -40°C .

Title Page

Abstract Introduction

Conclusions References

Tables Figures

◀ ▶

◀ ▶

Back Close

Full Screen / Esc

Printer-friendly Version

Interactive Discussion



Vapour isotopic composition in updrafts

M. Bolot et al.

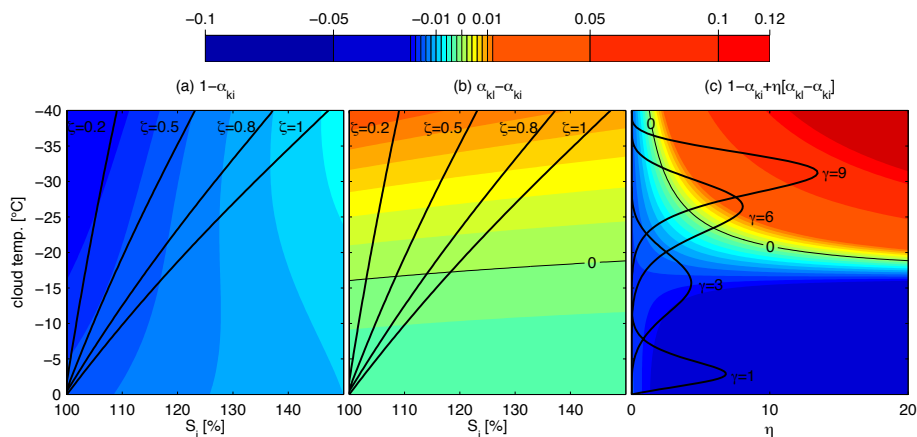


Fig. 6. Same as Fig. 5 but for the $\text{H}_2^{18}\text{O}/\text{H}_2\text{O}$ system. $\text{H}_2^{18}\text{O}/\text{H}_2\text{O}$ is more sensitive than $\text{HDO}/\text{H}_2\text{O}$ to kinetic effects, which means stronger fractionation limitation with ice supersaturation (panel **a**) and stronger re-enrichment in H_2^{18}O with the WBF effect (panel **b**), with onset of the re-enrichment at higher cloud temperature. A larger portion of the positive domain of $1 - \Lambda$ in panel **(c)** is sampled along the trajectories of η than for $\text{HDO}/\text{H}_2\text{O}$. Combining the effects of net moisture cooling and droplet evaporation, one can see that vapour is now re-enriched in heavy isotopologue when $\gamma = 6$ in addition to $\gamma = 9$, compared to the $\text{HDO}/\text{H}_2\text{O}$ system.

[Title Page](#)
[Abstract](#)
[Introduction](#)
[Conclusions](#)
[References](#)
[Tables](#)
[Figures](#)
[◀](#)
[▶](#)
[◀](#)
[▶](#)
[Back](#)
[Close](#)
[Full Screen / Esc](#)
[Printer-friendly Version](#)
[Interactive Discussion](#)


Vapour isotopic composition in updrafts

M. Bolot et al.

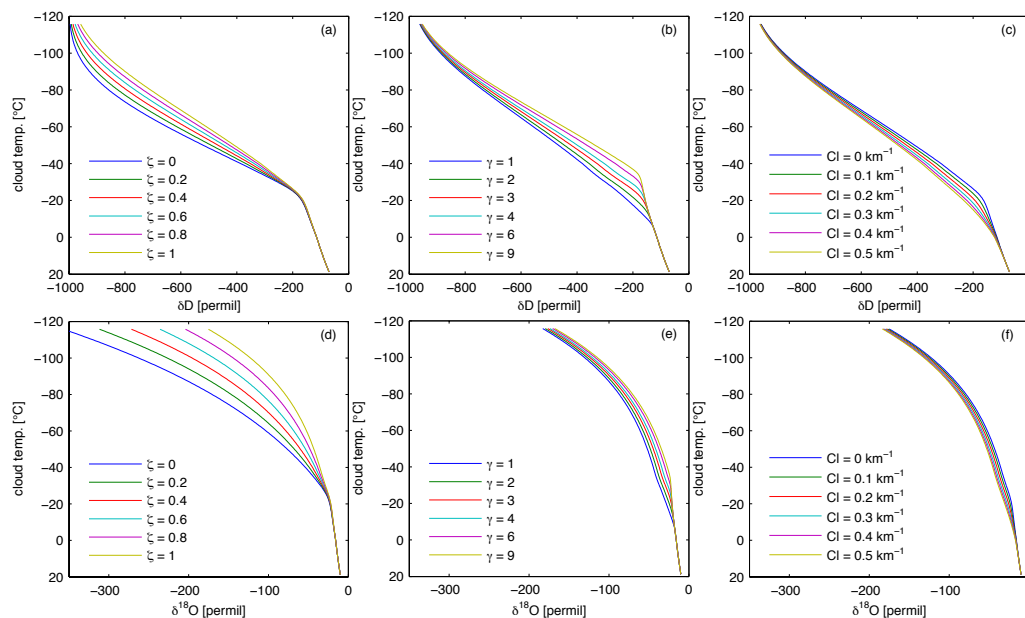


Fig. 7. Values of water vapour δD (a–c) and $\delta^{18}O$ (d–f) along cloud parcel temperature. (a, d) Sensitivity to the saturation parameter ζ . (b, e) Sensitivity to the glaciation parameter γ (glaciation temperature decreasing as γ increases, see Table 1). (c, f) Sensitivity to liquid water auto-conversion parameter C_l . Parameters not varied are taken from the default scenario of Sect. 4.

[Title Page](#)
[Abstract](#)
[Introduction](#)
[Conclusions](#)
[References](#)
[Tables](#)
[Figures](#)
[Back](#)
[Close](#)
[Full Screen / Esc](#)
[Printer-friendly Version](#)
[Interactive Discussion](#)


Vapour isotopic composition in updrafts

M. Bolot et al.

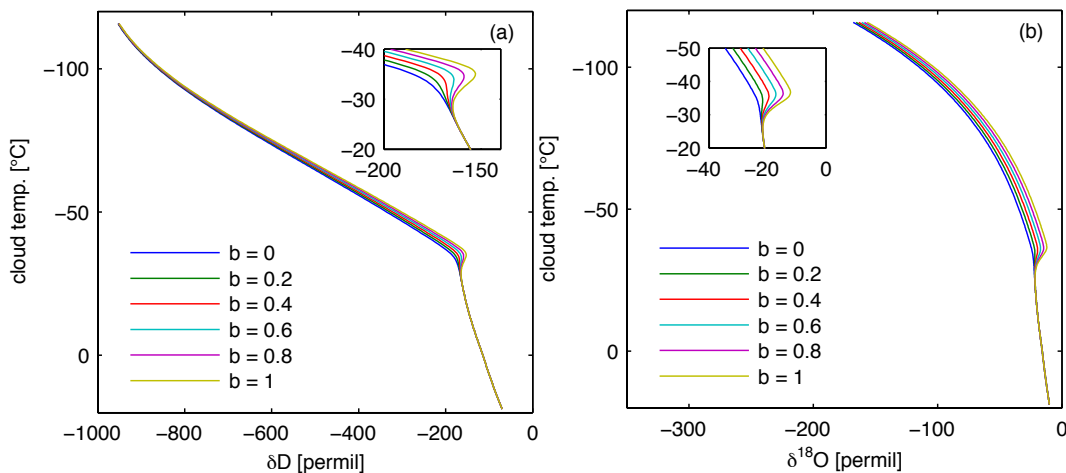


Fig. 8. (a) Sensitivity of δD along cloud parcel temperature to the WBF parameter b with the glaciation parameter $\gamma = 9$ (glaciation temperature -38°C). (b) Same as (a) for $\delta^{18}\text{O}$. Other parameters are taken from the default scenario of Sect. 4.

Title Page

Abstract

Introduction

Conclusions

References

Tables

Figures

◀

▶

◀

▶

Back

Close

Full Screen / Esc

Printer-friendly Version

Interactive Discussion



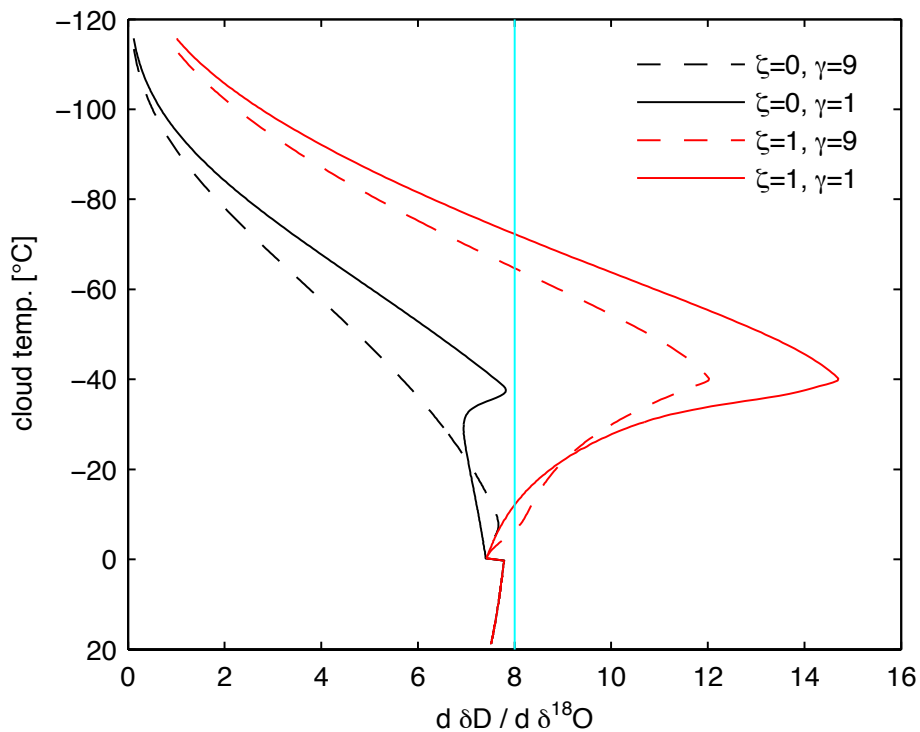


Fig. 9. Slope of δD versus $\delta^{18}O$ as a function of cloud parcel temperature for values of saturation and glaciation parameters (ζ and γ) indicated on the panel. The vertical line indicates the value 8 used in the definition of d-excess (when the slope of δD versus $\delta^{18}O$ equals 8, d-excess is conserved).

Vapour isotopic composition in updrafts

M. Bolot et al.

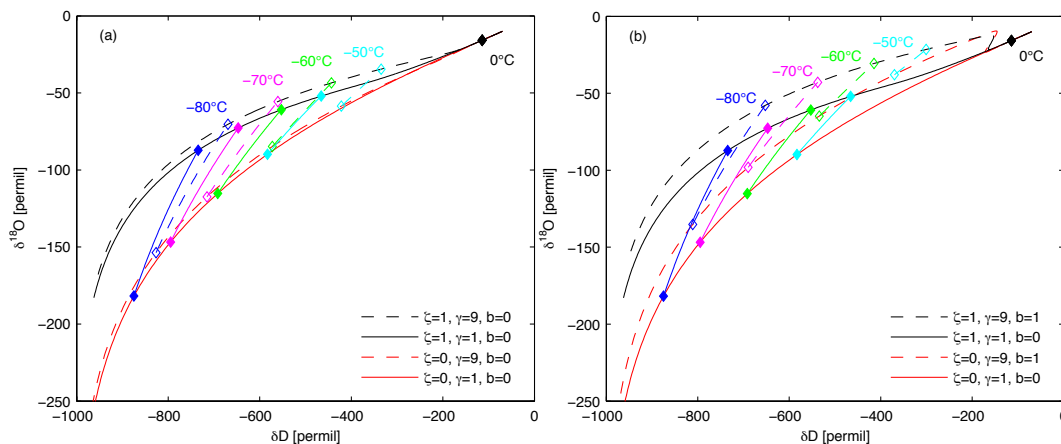


Fig. 10. (a) Sensitivity of the δD – $\delta^{18}O$ relationship to glaciation and saturation parameters γ and ζ . Glaciation proceeds as pure freezing ($b = 0$). **(b)** Same as **(a)** but glaciation proceeds as a pure WBF process ($b = 1$) when the glaciation parameter is $\gamma = 9$. Isotherm curves at -80°C , -70°C , -60°C and -50°C are shown for varying ζ from 0 to 1 under the following scenarios: $\gamma = 1$, $b = 0$ (solid lines, panels **a** and **b**), $\gamma = 9$, $b = 0$ (dashed lines, panel **a**), $\gamma = 9$, $b = 1$ (dash-dotted lines, panel **b**).

[Title Page](#)
[Abstract](#)
[Introduction](#)
[Conclusions](#)
[References](#)
[Tables](#)
[Figures](#)
[◀](#)
[▶](#)
[◀](#)
[▶](#)
[Back](#)
[Close](#)
[Full Screen / Esc](#)
[Printer-friendly Version](#)
[Interactive Discussion](#)


Vapour isotopic composition in updrafts

M. Bolot et al.

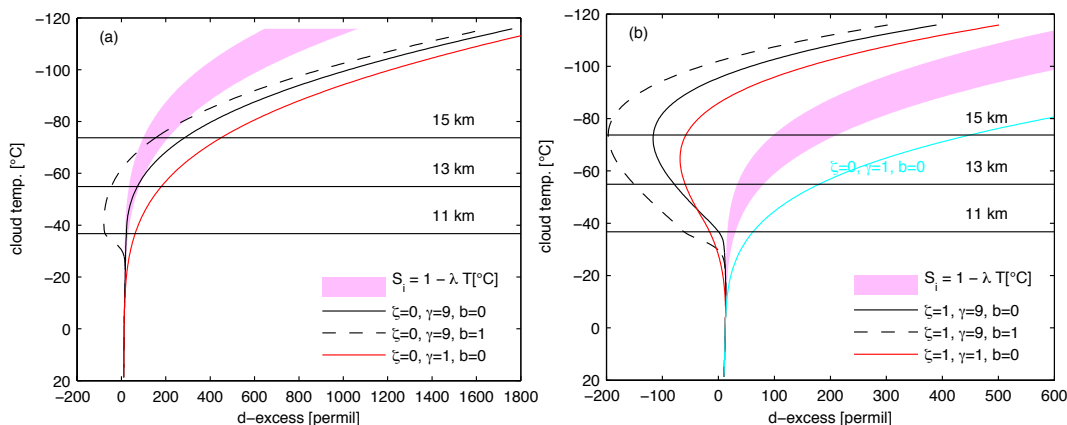


Fig. 11. (a) Deuterium excess values for conditions of equilibrium saturation over ice ($\zeta = 0$) and varying values of the glaciation and WBF parameters, γ and b , as indicated in the panel. Magenta area: range of d-excess values when the saturation is parameterized as $S_i = 1 - \lambda T$ [°C] where λ varies in the range $0.003 \text{ °C}^{-1} - 0.006 \text{ °C}^{-1}$, and the glaciation temperature is -15 °C ($\gamma = 1.5$). **(b)** Same as **(a)** except for conditions of equilibrium saturation over liquid water in the mixed-phase zone ($\zeta = 1$). The case $\zeta = b = 0$ and $\gamma = 1$ is reproduced from panel **(a)** in the sake of comparison.

[Title Page](#)
[Abstract](#)
[Introduction](#)
[Conclusions](#)
[References](#)
[Tables](#)
[Figures](#)
[◀](#)
[▶](#)
[◀](#)
[▶](#)
[Back](#)
[Close](#)
[Full Screen / Esc](#)
[Printer-friendly Version](#)
[Interactive Discussion](#)


Vapour isotopic composition in updrafts

M. Bolot et al.

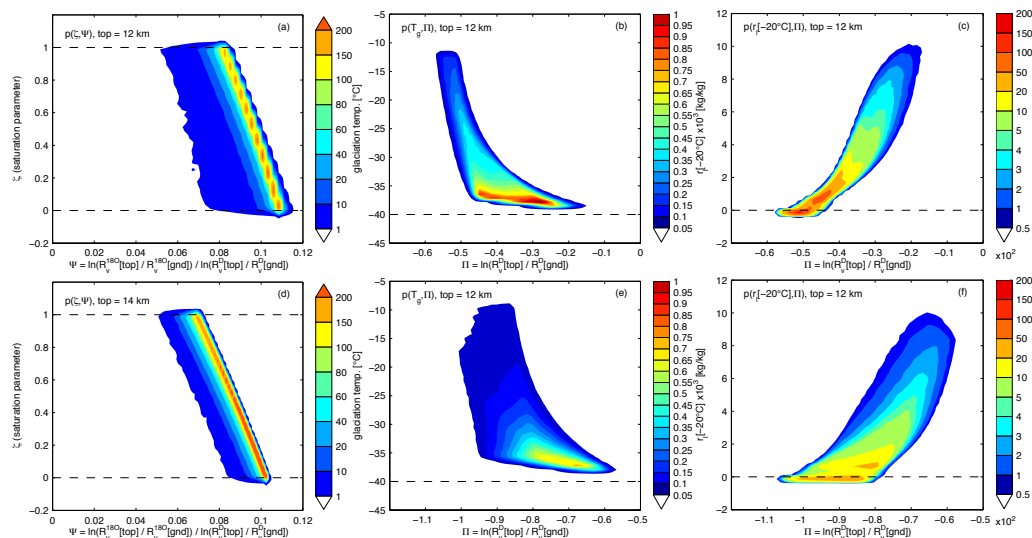


Fig. 12. First row: cloud top isotopic ratios ($R_V^D(\text{top})$, $R_V^{18O}(\text{top})$) taken at 12 km. **(a)**: values of the joint probability density $p(\zeta, \Psi)$ as a function of the saturation parameter ζ and $\Psi = \ln\left(\frac{R_V^{18O}(\text{top})}{R_V^{18O}(\text{gnd})}\right) / \ln\left(\frac{R_V^D(\text{top})}{R_V^D(\text{gnd})}\right)$. **(b)** Values of the joint probability density $p(T_g, \Pi)$ as a function of the glaciation temperature T_g and $\Pi = \ln\left(\frac{R_V^D(\text{top})}{R_V^D(\text{gnd})}\right)$. **(c)** Values of the joint probability density $p(r_1[-20^\circ\text{C}], \Pi)$ as a function of the supercooled liquid water content at -20°C $r_1[-20^\circ\text{C}]$ and Π . Second row **(d)**, **(e)** and **(f)**: same as first row **(a)**, **(b)** and **(c)** but for cloud top isotopic ratios taken at 14 km. $R_V^D(\text{gnd})$ and $R_V^{18O}(\text{gnd})$ are cloud base isotopic ratios.

Title Page

Abstract

Introduction

Conclusions

References

Tables

Figures

◀

▶

◀

▶

Back

Close

Full Screen / Esc

Printer-friendly Version

Interactive Discussion



Vapour isotopic composition in updrafts

M. Bolot et al.

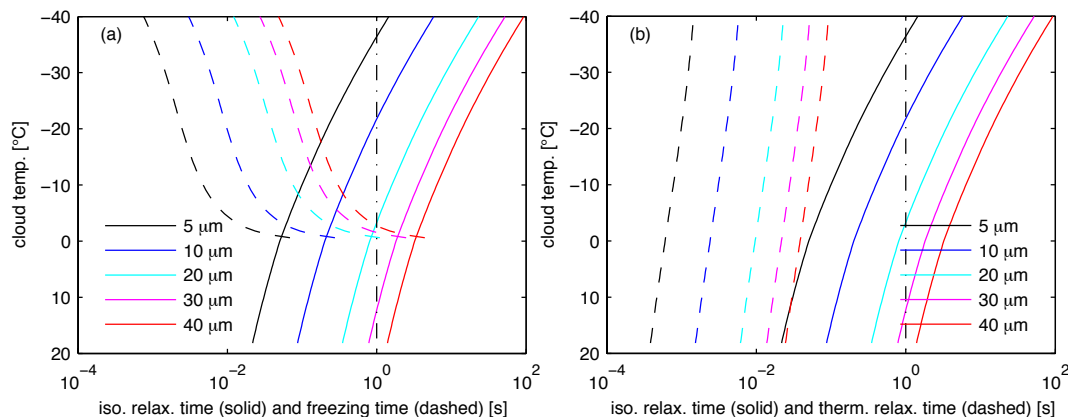


Fig. B1. (a) Isotopic relaxation time τ_{drop} (solid) and freezing time t_f (dashed) for droplets of varying radii. (b) Isotopic relaxation time τ_{drop} (solid) and thermal relaxation time t_h (dashed) for droplets of varying radii. The droplets are assumed to be spherical. Freezing time is computed following Eq. (D1) and thermal relaxation time follows Eq. (D2). Temperature, pressure and vapour saturation used in the computations are taken along a reference integration of the cloud model as described in Sect. 4. The vertical line is drawn for $\tau = 1$ s.

Title Page

Abstract

Introduction

Conclusions

References

Tables

Figures

◀

▶

◀

▶

Back

Close

Full Screen / Esc

Printer-friendly Version

Interactive Discussion

